Characterisation and trophic functions of murine embryonic macrophages based upon the use of a Csf1r-EGFP transgene reporter

Available online at www.sciencedirect.com
ScienceDirect
Developmental Biology 308 (2007) 232–246
DEVELOPMENTAL BIOLOGY
www.elsevier.com/locate/ydbio

Characterisation and trophic functions of murine embryonic macrophages based upon the use of a *Csf1r*–EGFP transgene reporter

Fiona Rae [a,1], Kyra Woods [a,1], Tedjo Sasmono [a,2], Naomi Campanale [b], Darrin Taylor [a], Dmitry A. Ovchinnikov [a,c], Sean M. Grimmond [a], David A. Hume [a,c], Sharon D. Ricardo [b], Melissa H. Little [a,*]

[a] *Institute for Molecular Bioscience and ARC Special Research Centre for Functional and Applied Genomics, University of Queensland, Brisbane, Queensland, 4072, Australia*
[b] *Monash Immunology and Stem Cell Laboratories, Monash University, Melbourne, Victoria, 3800, Australia*
[c] *Cooperative Research Centre for Chronic Inflammatory Diseases, Australia*

Received for publication 1 December 2006; revised 8 May 2007; accepted 22 May 2007
Available online 25 May 2007

Abstract

All solid organs contain resident monocyte-derived cells that appear early in organogenesis and persist throughout life. These cells are critical for normal development in some organs. Here we report the use of a previously described transgenic line, with EGFP driven by the macrophage-restricted *Csf1r* (*c-fms*) promoter, to image macrophage production and infiltration accompanying organogenesis in many tissues. Using microarray analysis of FACS-isolated EGFP-positive cells, we show that fetal kidney, lung and brain macrophages show similar gene expression profiles irrespective of their tissue of origin. EGFP-positive cells appeared in the renal interstitium from 12 days post coitum, prior to nephrogenesis, and maintain a close apposition to renal tubules postnatally. CSF-1 added to embryonic kidney explants increased overall renal growth and ureteric bud branching. Expression profiling of tissue macrophages and of CSF-1-treated explants showed evidence of the alternate, pro-proliferative (M2) activation profile, including expression of macrophage mannose receptor (CD206), macrophage scavenger receptor 2 (Msr2), C1q, CD163, selenoprotein P, CCL24 and TREM2. This response has been associated with the trophic role of tumour-associated macrophages. These findings suggest a trophic role of macrophages in embryonic kidney development, which may continue to play a similar role in postnatal repair.

Keywords: Embryonic macrophage; Expression profiling; Colony-stimulating factor 1 (CSF-1); *Csf1R*; *c-fms*; Kidney development; Organogenesis; EGFP transgene; Alternate macrophage activation

Introduction

During mammalian development, specialized phagocytic cells are formed in the yolk sac and rapidly infiltrate the embryo via the developing vasculature. As definitive haematopoiesis is established in the liver, a distinct set of phagocytes, the monocyte–macrophages of the adult, are formed (Lichanska et al., 1999; Lichanska and Hume, 2000; Shepard and Zon, 2000). A major function of phagocytic cells in development is to clear dying cells. Consequently, a lack of macrophages during this period causes developmental problems, especially in brain and lung (Henson and Hume, 2006; Li et al., 2005; Wood et al., 2000). In mammals, the production of macrophages by the liver, and subsequently by the bone marrow, is controlled in large part by the growth factor macrophage colony-stimulating factor (CSF-1). CSF-1 acts on its target cells by binding to colony-stimulating factor 1 receptor (*Csf1r*), a cell-surface tyrosine kinase receptor encoded by the *c-fms* proto-oncogene, which is expressed in macrophage and trophoblast cell lineages (Chitu and Stanley, 2006; Stanley et al., 1997; Sweet and Hume, 2003). *Csf1r* is critical for the proliferation, survival and differentiation of macrophages as disruption of the gene results in

* Corresponding author. Fax: +61 7 3346 2101.
E-mail address: m.little@imb.uq.edu.au (M.H. Little).
[1] Equal contribution was made by these authors.
[2] Current address: Eijkman Institute for Molecular Biology Jl., Diponegoro 69 Jakarta 10430, Indonesia.

0012-1606/$ - see front matter © 2007 Elsevier Inc. All rights reserved.
doi:10.1016/j.ydbio.2007.05.027

large depletions of macrophages in most tissues (Dai et al., 2002). Upon reaching a tissue compartment from the bloodstream, monocytes differentiate into resident tissue macrophages. Resident macrophage populations adapt to their local environment resulting in dramatically different phenotypes in different organs, for example Langerhans cells (skin), Kupffer cells (liver), microglia (brain) and osteoclasts (bone) (Gordon and Taylor, 2005; Hume, 2006).

The localization of *c-fms* (*Csf1r*) mRNA by whole mount *in situ* hybridization has been used to assess the appearance of embryonic phagocytes in the mouse yolk sac, and the subsequent onset of monocytopoiesis in the liver (Hume et al., 1995; Lichanska et al., 1999). The early embryonic phagocytes are distinct from adult macrophages in their expression of a number of key receptors, in their independence of the macrophage-restricted transcription factor, PU.1 (Lichanska et al., 1999), and the fact that they do not apparently arise through a classical monocyte intermediate (Lichanska and Hume, 2000). There are no mice that lack macrophages altogether, but the phenotypes of *c-fms*, CSF-1 and PU.1-mutant animals all imply that there are essential trophic roles played by these cells in the development of multiple organ systems (Cohen et al., 1996; Dai et al., 2002; Geutskens et al., 2005; Michaelson et al., 1996; Van Nguyen and Pollard, 2002). Macrophages are also implicated in tissue repair in adults. In models of acute damage to muscle, liver, lung, gastrointestinal tract and peripheral nervous system, infiltration by macrophages and production of macrophage-derived trophic factors, appears to be absolutely essential for regeneration (Abe et al., 2004; Berezovskaya et al., 1995; Kluth et al., 2004; Park and Barbul, 2004; Pull et al., 2005). However, macrophages are the classical two-edged sword. During chronic inflammation or a disease setting associated with severe progressive injury, macrophages are the dominant cell type implicated directly in cell death and tissue damage.

To gain an insight into the possible role of macrophages in development we have performed the first molecular profiling of these resident embryonic macrophages and have examined the effect of manipulation of their function *in vitro*. We have previously described a transgenic mouse in which the *Csf1r* promoter drives expression of an EGFP reporter gene (Sasmono et al., 2003). Here, we show that this reporter gene is expressed in, and restricted to, macrophage populations throughout development and recapitulates the previously reported expression pattern of *Csf1r* mRNA. We also show that the EGFP marker can be used to isolate macrophages from mouse embryos and that these cells have a distinctive mRNA expression profile. Finally, we demonstrate the potential trophic role of macrophages in organogenesis through administration of CSF-1 to renal explant cultures *in vitro*.

Materials and methods

Isolation and preparation of tissue for confocal analysis

All animal experimentation was approved by an institutional Animal Ethics Committee (AEEC3, University of Queensland). Male transgenic mice expressing either enhanced green fluorescence protein (EGFP) (Sasmono et al., 2003) or enhanced cyan fluorescent protein (ECFP) (Ovchinnikov, unpublished observations) driven from the *Csf1r* promoter were mated to CD1 outbred females. Pregnant females were sacrificed at 11.5, 12.5, 15 dpc and newborn. Transgenic offspring were determined by visualization of placental EGFP or ECFP expression. Transgenic tissues were dissected separately in ice-cold PBS, fixed in 4% paraformaldehyde (PFA) for 3 h, room temperature then equilibrated in 30% sucrose overnight at 4 °C before mounting in Tissue-Tek OCT medium in isopentane cooled over dry ice.

Immunofluorescence analysis

Light and confocal microscopy was used for fluorescence visualization of *c-fms*–EGFP–macrophages in kidneys from 11.5 dpc, 12.5 dpc, 13.5 dpc, 15.5 dpc, 18.5 dpc and adult tissue. Following 4% PFA fixation, frozen sections were cut at 5 μm using a cryostat (Leica, Bensheim, Germany) and visualized under an Olympus Provis AX70 fluorescent microscope. Immunofluorescence staining used the following antibodies; rat anti-mouse F4/80 (Serotec, Oxford, UK), rabbit anti-aquaporin-1 (Chemicon, Temecula, CA) and anti-mouse calbindin-D28K (Sigma Chemical Company, MI, USA). Where mouse primary antibodies were used, kidney sections were incubated with M.O.M.™ blocking diluent (Vector Laboratories, Burlingham, CA) before addition of primary antibody. Goat anti-rat Alexa Fluor 594, goat anti-rabbit Alexa Fluor 594, and goat anti-mouse Alexa Fluor 488 (all from Molecular Probes, Eugene, OR) were used to visualize F4/80, aquaporin-1 and calbindin, respectively. Sections were mounted with a fluorescent mounting media (DakoCytomation) before visualization with a Fluoview 1000 confocal microscope (Olympus, Tokyo, Japan), FV10-ASW software (version 1.3c; Olympus), step size at 0.5 μm when serial confocal microscopy analysis was applied.

Isolation of kidney, lung and brain embryonic tissue and macrophages

Tissues were harvested as above. 10–20 kidneys, 10 lungs or 10 brains were incubated in 1 ml Dissociation Media (1 mg/ml collagenase B, 1.2 U/ml dispase, 5 U/ml DNase II, in HANKS media) at 37 °C for 20 min. Organs were manually titrated with a P-1000 and incubated for a further 5 min at 37 °C. This step was repeated before the organs were dissociated with a 23-gauge syringe and passed through a 40 μM cell strainer (BD Bioscience). An equal volume of ice-cold PBS was washed through the strainer and the cells were centrifuged at 3000 rpm for 5 min. The supernatant was discarded and the cells resuspended in 2–3 ml of ice-cold PBS. Cells were passed again through a 40-μm cell strainer, checked under a microscope to ensure they were a single-cell suspension, and stored on ice ready for fluorescence activated cell sorting (FACS). Isolation of EGFP positive macrophages was carried out on a FACSVantage SE DiVa flow cytometer (BD Biosciences). Approximately 200 transgenic kidneys/100 lungs/100 brains were subjected to FACS analysis with non-transgenic littermate kidneys used as a reference. Isolated macrophages were washed with ice-cold PBS and stored at −70 °C in preparation for RNA extraction. Samples of aliquoted cells were routinely re-run through the FACS machine to confirm purity and the GFP+ status of the cells. Animal experimentation was covered by Animal Ethics Committee number IMB/479/03/NIH.

Immunophenotypic confirmation of the specificity of the Csf1r–EGFP reporter

To examine the specificity of the *Csf1r*–EGFP reporter, immunophenotypic analysis of the GFP-positive cells isolated using FACS from postnatal *Csf1r*–EGFP kidneys was performed. This analysis showed that 100% of the cells were positive for both EGFP and CD45 and up to 75% of the cells were positive for both EGFP and F4/80, which is present on a major sub-population of the *Csf1r*-positive monocytic fraction in the mouse embryo (Lichanska et al., 1999). Only 0.02% of the GFP+CD45+ cells were CD11c+, suggesting a very low number of GFP+ dendritic cells. We have also used two pericyte markers, monoclonal anti-α-smooth muscle actin Cy3 conjugate (Sigma-Aldrich, St Louis, MO; 1:1000 dilution) and CD31–APC conjugate (PharMingen, BD Biosciences, USA), to show that the GFP+ cells are not pericytes. These results suggest that there is limited heterogeneity and that the majority of the cells isolated based on EGFP expression are monocytic.

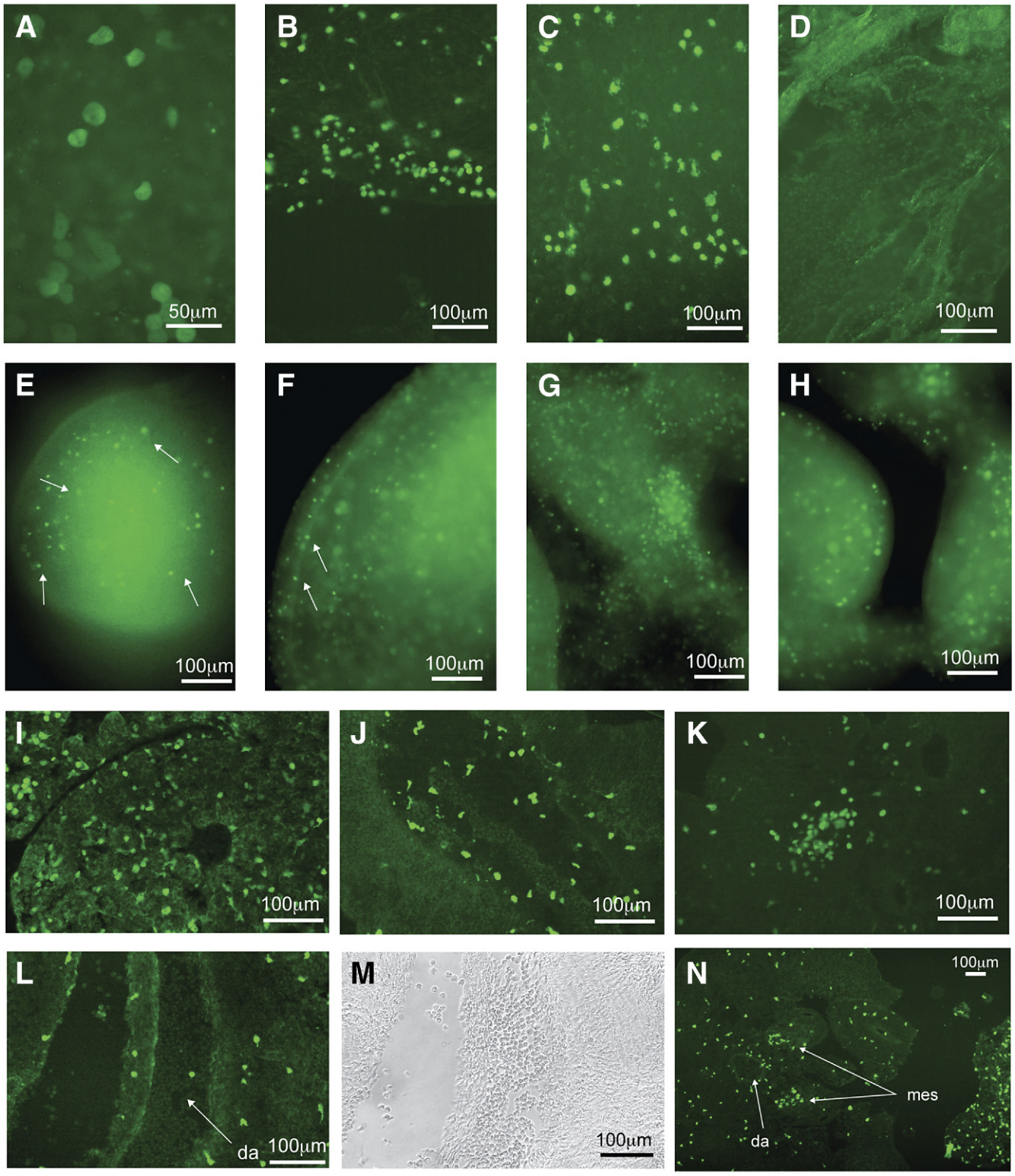

Fig. 1. Examination of transgene expression in yolk sac and embryo proper. (A–D) Whole mounts of yolk sacs from conceptuses at 9.5 dpc (A), 10.5 dpc (B) and 12.5 dpc (C). No green fluorescent cells could be observed in wildtype yolk sacs shown at 12.5 dpc (D). (E–N) Transgene expression in the embryo proper. Panel E shows the presence of EGFP-positive cells (arrows) in the limb bud of the 9.5 dpc embryo. A whole mount examination of 10.5 dpc embryos observed the presence of EGFP-positive cells throughout the body, such as shown in the dorsal area of the embryo (F), around the umbilical cord (G) and in the mandibular arches (H). In 10.5 dpc embryo sections, green fluorescent cells were prominent in the liver (I), developing brain (J) and in the thymus area (K). EGFP-expressing cells were detected in the aorta–gonad–mesonephros (AGM) area. Fluorescent (L) and bright field (M) images of sagittal sections through the dorsal aorta (da) of the 10.5 dpc embryo revealed EGFP-positive cells. More prominent accumulation of green fluorescent cells was apparent in the transverse section through the AGM area of an 11.5 dpc embryo (N), particularly in the mesonephric tubules (mes).

RNA extraction, amplification and microarray profiling

Total RNA was isolated using an RNeasy Mini Kit (Qiagen). RNA was subject to one round of amplification using the Amino Allyl MessageAmp RNA Kit (Ambion) as previously described (Challen et al., 2005). Briefly, 5 μg of control kidney, lung or brain tissue and 1.2 μg of macrophage total RNA was reverse-transcribed into cDNA using a T7 Oligo(dT) primer. *In vitro* transcription was then performed to generate antisense RNA (aRNA) containing amino allyl UTP nucleotide in place of UTP. The integrity of the aRNA was assessed by agarose gel electrophoresis and quantified by spectrophotometry. 5 μg of each sample was labeled via a coupling reaction using Cy3- or Cy5-reactive dyes (Amersham Biosciences). Following fragmentation of the labelled probe, hybridization to microarray slides was performed at 42 °C for 18 h. Each pairwise comparison (e.g. kidney macrophage vs. kidney; kidney macrophage vs. brain macrophage) experiment was performed in triplicate, including a dye reversal replicate. Compugen murine oligonucleotide microarray chips (22K elements, 65-mer oligos, visit http://www.labonweb.com/chips/libraries.html) were printed at the SRC Microarray Facility, University of Queensland (http://microarray.imb.uq.edu.au). Data values of gene expression levels were uploaded into BASE 1.2.10 and normalized. Genes were then analysed using a *B*-score statistic whereby genes with a *B*-score >0 have a >50% probability of being differentially expressed.

RNA in situ hybridization

Section RNA *in situ* hybridization was performed as previously described (Roche DIG Application Manual; 31) with minor modifications. Sections were dehydrated through an ethanol series prior to hybridization overnight at 65 °C. Post-hybridization washes consisted of 6×SSC (5 min, 65 °C), 2×SSC/50% formamide/10 mM EDTA (30 min, 65 °C), 2×SSC (2×30 min, 65 °C) and 0.2×SSC (2×30 min, 65 °C).

Kidney explant culture

Metanephric organ culture was used to test the effects of CSF-1, CCL4 and CCL9, CCL6, Cxcl1 and Gas6 on the developing metanephros. Metanephroi from 11.5 dpc mice were grown for 1–4 days on Poretics 13-mm polycarbonate inserts (Osmonics Inc.) with a membrane pore size of 1.0 μm at 37 °C with 5% CO_2 in 300 μl of DMEM/Hams F12 media (Invitrogen) supplemented with 50 μg/ml transferrin and 20 mM glutamine. Recombinant CSF-1 (Chiron) was added to a final concentration of 100 U/μl with LPS at (0.1–10 ng/ml). CCL4, CCL9, CCL6, Cxcl1, Gas6 (R&D Systems) were added at between 5 and 500 ng/ml. Data is presented for CSF-1 at 100 ng/ml. Co-immunofluorescence for calbindin-D28K (Sigma Chemical Company) and WT1 (Santa Cruz, SC-192) was performed to visualize the ureteric epithelium and early nephrons respectively, as previously described (Piper et al., 2002). Digital images were captured using a Dage "MTI" peltier cooled charge coupled device digital camera attached to an AX70 Olympus microscope, and processed using Adobe Photoshop 7 software. To semi-quantitatively assess the effects of these factors on *in vitro* metanephric development, branch tips and WT1-positive bodies (forming nephrons) present in each explanted metanephros were counted. Experiments were repeated at least twice with a total of between 8 and 10 metanephroi per experiment. As there is considerable variation between different litters in the stage of metanephric development present at isolation, a representative set of data from one experiment is presented with error bars representing the ±standard error of the mean. A one-way ANOVA followed by a Tukey's post-hoc test was used to assess significance.

Results

Population of the developing mouse with Csf1r–EGFP expressing cells

In the original description of the *Csf1r–EGFP* transgene, there was a limited examination of the expression in the embryo (Sasmono et al., 2003). Figs. 1–3 demonstrate that the EGFP reporter provides a unique and convenient marker for the appearance of macrophages during mouse embryonic development. EGFP-positive cells were first detectable in the yolk sac around 9–9.5 dpc (Figs. 1A–D). There was no obvious clustering of these cells around blood islands or any other structure, consistent with earlier reports that the yolk-sac-derived macrophages do not arise from conventional monocytopoiesis (Lichanska and Hume, 2000). At 9–9.5 dpc, the first EGFP-positive cells were also observed in the embryo proper (Figs. 1E–N). This was followed by a very rapid wave of migration occurring within a 24-h window. The numbers of EGFP-positive cells, their morphology and distribution in the yolk sac remain relatively constant through to 15.5 dpc, the latest time point examined. During embryonic haematopoiesis, the aorta–gonad–mesonephros (AGM) region becomes populated with haematopoietic progenitors (Dzierzak, 2003; Yoder, 2001). In 10.5 dpc embryos, sagittal sections through the dorsal aorta and its vicinity revealed the first EGFP-positive cells (Figs. 1L–N), some scattered within the mesenchyme and others present in the lumen of the aorta amongst the red blood cells, suggesting that they are arriving via the circulation. By 11.5 dpc, a transverse section clearly revealed the accumulation of clusters of fluorescent cells, particularly associated with the mesonephric tubules (Fig. 1N). The extensive infiltration of this region by EGFP-positive cells was especially evident in whole mounts of the 11.5 dpc genital ridge and dorsal aorta (Fig. 2D). Morphologically, cells in this region appeared smaller and more rounded than the stellate macrophages of the yolk sac and other parts of the embryo. As *Csf1r* is expressed on pluripotent progenitors cells (Tagoh et al., 2002), we suggest that the EGFP reporter is providing a unique marker for the macrophage population of the AGM. Progenitor cells in this region differ from those in fetal liver and adult in that they lack CD45 (Bertrand et al., 2005a), but their expression of *Csf1r* has not been reported. Elsewhere in the embryo, EGFP-positive cells were already a prominent population by 10.5 dpc (Figs. 1F–K). They were especially numerous and ramified in the developing brain (Fig. 1J), mandibular arches (Fig. 1H) and thymic anlage (Fig. 1K).

By 11.5 dpc, a high density of cells clustered around the reticulating vasculature of the head (Figs. 2A, B). Fig. 2C shows the continued increase in the developing limb. By the time the first large-scale cell death is observed, EGFP-positive cells appear concentrated under the apical ectodermal ridge (Fig. 2C) and in the anterior necrotic zone (not shown). In the AGM, there is a dense cluster of EGFP-positive cells (Fig. 2D). Fig. 2E shows the large numbers of macrophages that infiltrate the developing lens at this stage of embryonic development (Nishitani and Sasaki, 2006). Based upon the proportional area of any section that is positive for the marker, we estimate that EGFP-positive cells represent 3–10% of total cells in most parts of the embryo at this stage of development. At 13.5 dpc (Figs. 2G–L), a striking concentration of *Csf1r–EGFP*-positive cells was observed in the thymic anlage (Fig. 2H). There is little published work on myeloid population of the thymus at this early development stage, although the role of macrophages in

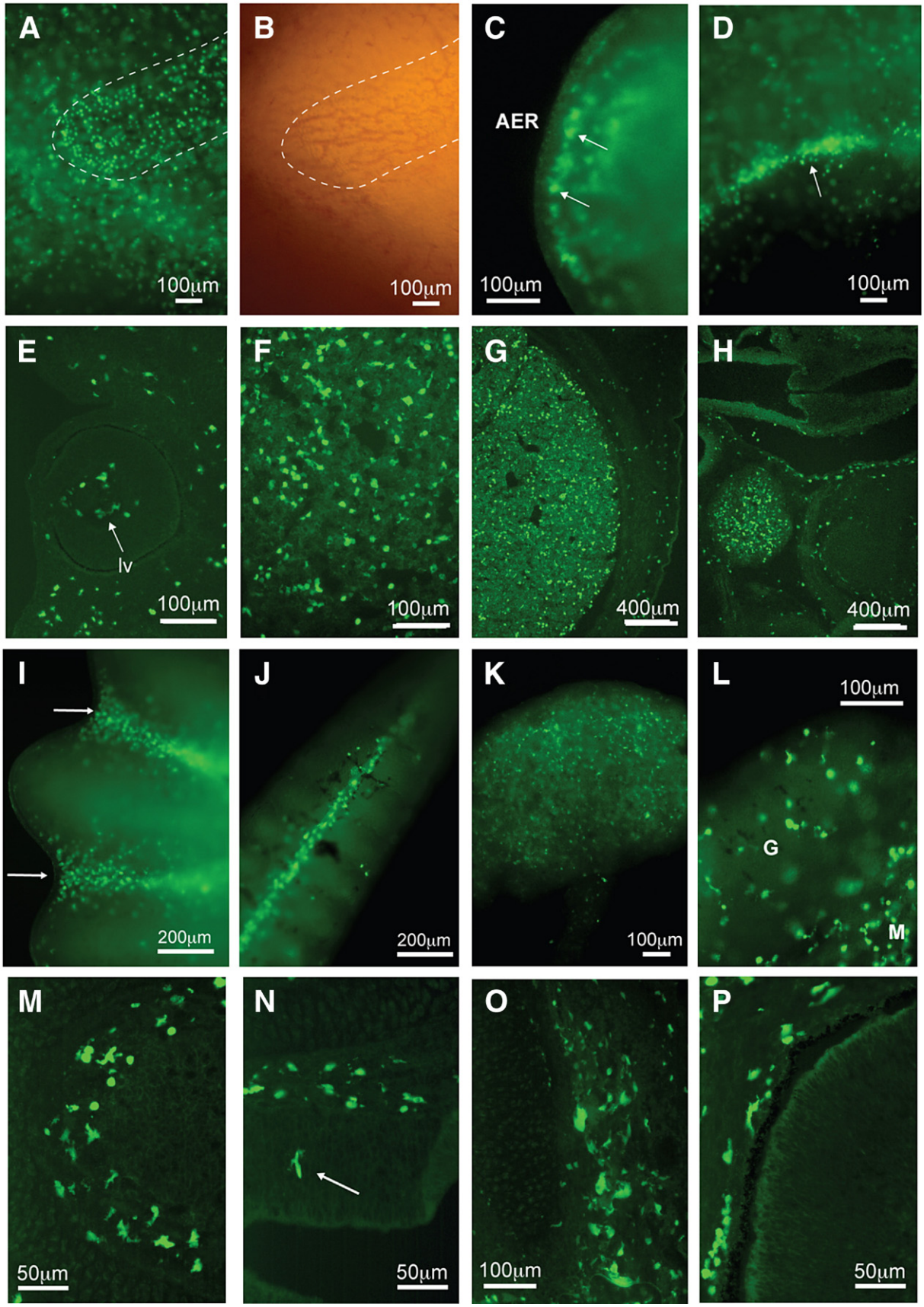
A
100μm
B
100μm
C
AER
100μm
D
100μm
E
lv
100μm
F
100μm
G
400μm
H
400μm
I
200μm
J
200μm
K
100μm
L
100μm
G
M
M
50μm
N
50μm
O
100μm
P
50μm

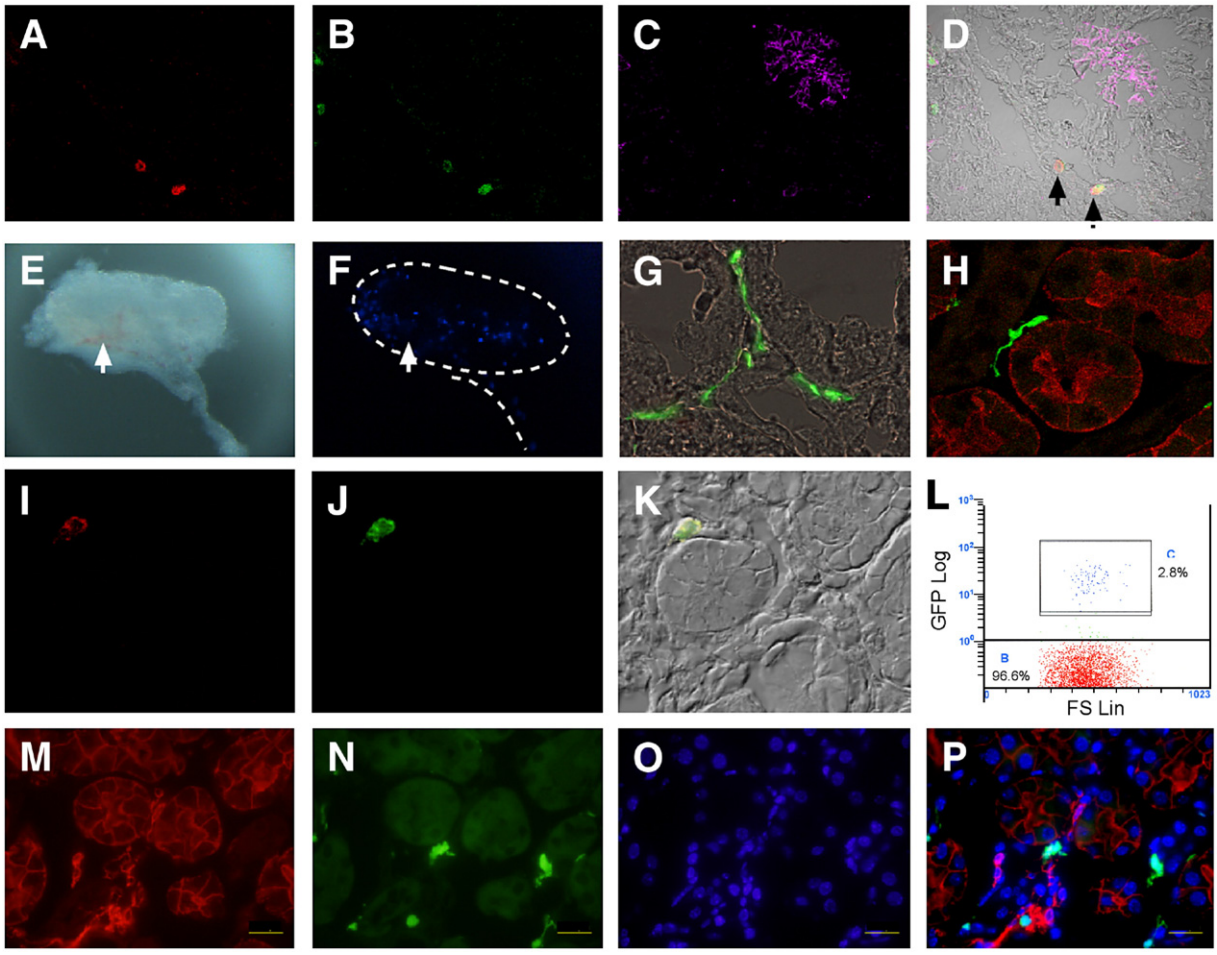

Fig. 3. Analysis of the arrival and final location of EGFP-positive cells in the permanent kidney (metanephros). (A–D) Confocal analysis of sections of 12.5 dpc mouse kidney showing expression of the macrophage marker F4/80 (A, red), EGFP (B, green), calbindin 28 kDa (C, pink) and a merge of these three channels with a bright field image of the same section (scale bar = 300 μm). Calbindin 28 kDa indicates the location of the ureteric bud. Black arrows indicate macrophages positive for both F4/80 and EGFP (D). (E, F) Whole metanephroi dissected from 11.5 dpc *Csf1r–ECFP* transgenic mice shown both as bright field (E) and fluorescence images (F, detecting ECFP). A dotted line shows the outline of the metanephros and the location of the ureter. Developing vasculature can be seen along the metanephros (white arrows), showing the relative location of the macrophages to the circulation (F). Localization of resident macrophages in the adult kidney. (G) Bright field with EGFP fluorescence overlay of section of adult kidney cortex showing macrophages between the tubules. (H) Immunolocalization of aquaporin-1 to proximal tubular epithelial cells (red) and EGFP overlay of adult kidney cortex showing the relative location of the resident macrophage in relationship to the proximal tubules by confocal microscopy. (I–K) Immunofluorescence of E16 mouse kidney showing EGFP (I), F4/80 (J) and a merge (K) illustrating the coexpression of the F4/80 macrophage marker with the EGFP transgene expression. (L) FACS-based isolation of renal macrophages from the 15.5 dpc kidneys of *Csf1r–EGFP* mice showing that EGFP-positive cells in the transgenic animals represents 2.8% of the total. (M–P) Three colour light microscopic analysis of the adult kidney showing immunofluorescence for aquaporin-1 (M, red), fluorescence of EGFP-positive macrophages (N, green), DAPI-stained nuclei (O, blue), and a merged image (P).

thymocyte phagocytosis later in development is clear (Anderson et al., 2000; Henson and Hume, 2006). The exceptionally high density of *Csf1r–EGFP* positive cells in the thymic anlage prior to the arrival of T lymphocytes clearly implicates these cells as key players in the development of the thymus. There is also a striking infiltration in the vicinity of the olfactory

Fig. 2. (A–F) *Csf1r–EGFP* in 11.5 dpc embryos. On examination of whole mount embryos, numerous EGFP-positive cells were distributed throughout the body, such as shown in the superficial tissues of the head with prominent green cells clustered around the blood vessels (A, dashed line) which could be seen in bright field (B, dashed line). Numerous green cells could be seen in the limb bud (C, arrows) with a strong accumulation evident under the apical ectodermal ridge (AER). Many cells in the AGM were also EGFP-positive (D, arrow). Panel E shows a section through the 11.5 dpc lens vesicle (lv). An embryo section through the liver (F) shows accumulation of green fluorescent cells. (G–L) EGFP examination in 13.5 dpc embryos. Extensive accumulation of EGFP-positive cells could be seen evenly distributed in the parenchyma of the liver (G) and the thymus area (H). Embryonic phagocytes are well known for their role in clearance of apoptotic cells as occurs in the interdigital areas of the developing footplate. In whole mounts of *Csf1r–EGFP* embryos, extensive accumulations of EGFP-positive cells were clearly observed in these regions (I, arrows). These cells could also be seen in the tail vein (J). In cultured organs, green fluorescent phagocytes were seen in the kidney (K) and ovary (L). G, developing gonad; M, mesonephros. (M–P) Examination of 15.5 dpc embryo sections. Panel M shows the nasal septum region, showing the EGFP-positive cells concentrated in the mesenchymal tissue separating the nasal septal cartilage and the olfactory epithelium. In some areas, green fluorescent cells infiltrated the olfactory epithelium (arrow, N). In the embryo, osteoclasts expressed EGFP, as shown around the humerus (O). In the developing eye, EGFP-expressing cells were prominent in the choroid layer beneath the pigment layer of the retina (P).

epithelium (Figs. 2M, N), which has emerged as a possible source of adult stem cells. Our observation suggests that the claim that haematopoietic stems cells are unlikely to be found in this location (Murrell et al., 2005) should be viewed with caution. Additional images from later stages of development (12.5 dpc, 13.5 dpc, 15.5 dpc) can be viewed on our web site at www.macrophages.com.

Macrophage recruitment in response to CSF-1 has been shown to have an essential function in the ductal outgrowth in the developing mammary gland (Van Nguyen and Pollard, 2002). To look for additional roles of infiltrating macrophages during organogenesis, we focused on another well-studied example of branching morphogenesis, the developing kidney. In the kidney, organogenesis involves the infiltration of the metanephric mesenchyme by the ureteric bud and subsequent branching morphogenesis and mesenchymal-to-epithelial transition to produce a functional nephron (Saxen, 1987). Using confocal analysis of kidneys from the *Csf1r–EGFP* mice, EGFP-positive cells were first detected within the kidney between 11.5 and 12 dpc (Figs. 3A–F) and infiltrated the renal interstitium. Figs. 3A–D demonstrates the co-localization of F4/80, a marker of mature macrophages, in EGFP-positive cells in the interstitium surrounding the ureteric bud. Using *Csf1r–ECFP* mice, which have a higher level of fluorescence, *ECFP*-positive cells surrounding the dissected 11.5 dpc metanephros appeared to be closest to the developing vascular bed between the metanephric mesenchyme and the metanephric duct (Figs. 3E, F), suggesting that the macrophages enter the renal mesenchyme from or with the circulation at around this time. As the tubules of the developing nephrons arise and the interstitial space contracts, the renal macrophages become intimately associated with the basement membranes of the adjacent proximal and distal tubules (Figs. 3G–K). Their cellular processes wrap around neighbouring tubules facilitating an intimate relationship with the cells of these tubules. A 3D reconstruction of Fig. 3H showing this relationship can be seen at http://kidney.scgap.org/files/CSF1_Supp_Data/3D_reconstruction/Fig.%203H.avi.

Characterising expression profile of embryonic macrophage populations

Macrophages of the developing embryo are known to have a distinct gene expression profile compared to adult (Lichanska et al., 1999; Lichanska and Hume, 2000). The EGFP marker, and the comparative abundance of the EGFP-positive cells, makes it feasible to sort the embryonic macrophages from individual tissues to perform expression profiling. To address the question of whether macrophages in particular organs perform an organ-specific function, or adapt to a particular developmental niche, we compared the profiles of resident embryonic kidney, lung and brain EGFP-positive cells isolated from 15.5 dpc murine embryos using FACS separation. The relative abundance of macrophages was similar for all three tissues, with the EGFP-positive population representing approximately 2–5% of the total cells of all organs analysed (kidney shown in Fig. 3L) at 15.5 dpc. Initial expression profiling using 16,000 element Compugen oligonucleotide arrays was performed as a direct three-way comparison between E15.5 kidney-derived, lung-derived and brain-derived GFP-positive cells in order to determine the homogeneity of the resident embryonic monocytic phenotype at this time point. The primary data for these experiments can be viewed using BASE at http://kidney.scgap.org/base (username: devbiolreviewer; password: csf1). The data has also been placed on GEO (Accession no. GSE6271). A complete table showing the results of can be found at http://kidney.scgap.org/CSF1_Supp_Data/Macrophage_summary/Supp_table1.xls. An analysis of the genes identified as distinguishing between any two populations revealed that the only differences seen represented genes known to be highly specific for the organ of origin. Hence, kidney outliers compared to brain and lung included cadherin 16 and WT1, both known to be highly enriched in kidney. Similarly, outliers in brain included the microtubule-associated protein tau, tubulin alpha 1 and neuronatin while outliers in lung included surfactant protein C and fibrillin 1. This implied that the only significant differences between resident embryonic macrophages resulted from minor contamination with the source tissue or the presence of RNA from other cells types in macrophages post phagocytosis.

To verify the similarity in expression pattern of resident embryonic macrophages from different tissues, expression profiling of kidney versus EGFP-enriched kidney macrophages, brain versus brain macrophages and lung versus lung macrophages was performed using 16,000 element Compugen oligonucleotide arrays. This analysis was internally validated in each case by the fact that the *Csf1r* mRNA was enriched in the EGFP-positive population. A complete table showing the results of can be found at http://kidney.scgap.org/CSF1_Supp_Data/Macrophage_summary/Supp_table2.xls. The primary data for these experiments can be viewed using BASE at http://kidney.scgap.org/base (username: devbiolreviewer; password: csf1; GEO Accession no. GSE6271). Table 1 lists the 50 genes showing the highest enrichment ratio comparing the EGFP-enriched and parent tissue in each of the organs analysed. The relative enrichment of *Csf1r* expression itself was 5.4-, 2.8- and 7.6-fold in the kidney, lung and brain, respectively. This unexpectedly low enrichment may suggest that *Csf1r* mRNA is expressed, albeit at much lower levels than in macrophages, in other cells of the kidney. Table 2 lists the 50 genes for which the statistical confidence of the differential gene expression (*B*-statistic) was highest. For all three macrophage populations, *Csf1r* showed a *B*-score in the top 50 (6.97, 3.72, 6.64 for kidney, lung and brain) demonstrating that the FACS-based enrichment for cells expressing this gene is highly robust (*B*-score of >0 is statistically significant). The gene expression analysis performed on the three resident macrophage populations showed extremely high concordance (Tables 1 and 2). There were no genes that were unequivocally enriched in the EGFP-positive fraction in any one organ compared to another suggesting that the foetal macrophage phenotype is very similar between organs. In contrast, the genes enriched in the parent tissues (kidney, lung, and brain) were clearly tissue-specific as would be expected (see Table 1, right panel).

Table 1
A comparison of the genes demonstrating the highest fold change between macrophage and tissue of origin

Kid M V Kid	lung M V Lung	brain M V Brain	Gene name / Accession number
28.2	39.1	3.2	C-type lectin domain family 7, member a
25.1	22.9	9.1	Dual specificity phosphatase 1
20.4	7.5	4.2	Regulator of G-protein signaling 1
15.0	3.4	4.6	FYN binding protein
14.0	13.6	3.3	Leukocyte Ig-like receptor, subfamily B, member 4 (Gp49a)
13.2	3.6	6.7	Membrane-spanning 4-domains, subfamily A, member 6B
13.1	13.1	6.8	CD52 antigen
13.0	2.3	1.5	Stefin A3
12.8	1.6	1.5	Chemokine (C-X-C motif) ligand 1
12.4	4.9	2.6	G-protein coupled receptor 65
11.8	16.3	3.1	B-cell leukemia/lymphoma 2 related protein A1d
11.6	4.3	6.4	Fc receptor, IgE, high affinity I, gamma polypeptide
11.6	6.3	20.0	Mannose receptor, C type 1
11.5	15.8	5.0	Chemokine (C-C motif) ligand 6
11.1	21.0	8.6	Chemokine (C-X-C motif) ligand 2
11.0	13.5	9.2	P lysozyme structural
11.0	12.0	6.3	CD14 antigen
11.0	2.1	2.5	Regulator of G-protein signaling 2
10.6	17.9	12.8	Splicing factor 3b, subunit 3
10.6	3.2	11.6	F4/80
10.6	3.9	4.9	Lysozyme
10.6	8.1	1.9	Interleukin 1 beta
10.5	9.5	4.3	S100 calcium binding protein A8 (calgranulin A)
10.1	5.3	9.6	Macrophage expressed gene 1
10.0	6.4	6.1	Transferrin
9.9	9.3	6.2	Chemokine (C-C motif) ligand 9
9.6	6.8	11.1	Chemokine (C-C motif) ligand 4
9.1	7.9	5.9	transferrin, segment 4
9.1	7.9	1.8	Complement component 3
8.9	4.6	9.6	Lymphocyte antigen 86
8.8	2.3	3.1	C-type lectin domain family 4, member a2
8.7	3.5	3.2	Allograft inflammatory factor 1
8.7	2.2	3.1	Immunoglobulin superfamily, member 6
8.6	17.6	10.4	Lysosomal-associated protein transmembrane 5
8.6	3.7	8.8	Apolipoprotein E
8.6	9.5	6.7	Glia maturation factor, gamma
8.3	2.1	3.5	CD86 antigen
8.3	1.6	6.9	CD163 antigen
8.3	6.1	3.1	Phorbol-12-myristate-13-acetate-induced protein 1
8.2	2.8	4.3	Membrane-spanning 4-domains, subfamily A, member 11
8.1	5.9	9.4	Chemokine (C-C motif) ligand 2
8.0	12.9	6.9	FBJ osteosarcoma oncogene B
7.9	11.1	9.7	Fc receptor, IgG, low affinity III
7.9	24.3	7.1	signal-regulatory protein alpha (Sirpa)
7.9	2.9	4.0	Transferrin
7.8	3.8	1.2	ST8 alpha-N-acetyl-neuraminide alpha-2,8-sialyltransferase 4
7.7	7.7	3.8	Interferon regulatory factor 5
7.5	2.7	4.0	Chemokine (C-C motif) ligand 12
7.5	6.7	2.4	B-cell leukemia/lymphoma 2 related protein A1d
7.4	3.6	9.8	Macrophage scavenger receptor 2

Kid M V Kid	lung M V Lung	brain M V Brain	Gene name / Accession number
28.2	39.1	3.2	C-type lectin domain family 7, member a
7.9	24.3	7.1	signal-regulatory protein alpha (Sirpa)
25.1	22.9	9.1	Dual specificity phosphatase 1
11.1	21.0	8.6	Chemokine (C-X-C motif) ligand 2
2.3	20.3	2.1	AF357461
10.6	17.9	12.8	Splicing factor 3b, subunit 3
8.6	17.6	10.4	Lysosomal-associated protein transmembrane 5
7.1	17.3	5.5	CD83 antigen
11.8	16.3	3.1	B-cell leukemia/lymphoma 2 related protein A1d
11.5	15.8	5.0	Chemokine (C-C motif) ligand 6
1.3	15.7	3.8	Mouse 28S large subunit rRNA
2.9	15.1	4.2	M93319
14.0	13.6	3.3	Leukocyte Ig-like receptor, subfamily B, member 4 (Gp49a)
11.0	13.5	9.2	P lysozyme structural
13.1	13.1	6.8	CD52 antigen
8.0	12.9	6.9	FBJ osteosarcoma oncogene B
1.8	12.2	1.9	X81439
1.9	12.1	2.9	NADH dehydrogenase chain 5
11.0	12.0	6.3	CD14 antigen
6.9	11.8	4.5	Gem-interacting protein
2.2	11.5	3.0	BC004015
1.7	11.2	3.2	3′ end of mouse 18S ribosomal RNA
7.9	11.1	9.7	Fc receptor, IgG, low affinity III
4.1	10.6	4.8	Immediate early response 3
5.6	10.2	10.4	4.5S small RNA associated with poly-(a)-containing RNAs
6.5	10.1	2.0	B-cell leukemia/lymphoma 2 related protein A1c
1.6	10.1	1.9	c-Maf protein {proto-oncogene}
1.7	10.1	2.6	NADH dehydrogenase 1, mitochondrial
1.0	9.9	2.1	RIKEN cDNA 1810013D10 gene
5.1	9.8	1.6	Pleckstrin homology, Sec7 and coiled-coil domains, binding protein
6.1	9.6	2.7	Coiled-coil domain containing 88
10.5	9.5	4.3	S100 calcium binding protein A8 (calgranulin A)
8.6	9.5	6.7	Glia maturation factor, gamma
6.0	9.4	7.8	U3B small nuclear RNA 4
9.9	9.3	6.2	Chemokine (C-C motif) ligand 9
1.1	9.2	2.0	Interleukin 12a
1.0	9.1	8.2	S100 calcium binding protein A9 (calgranulin B)
1.2	9.0	1.8	POU domain, class 4, transcription factor 2
5.1	8.9	1.4	S100 calcium binding protein A4
1.4	8.9	2.2	Expressed sequence AU017263
1.3	8.9	1.7	RIKEN cDNA 4931433A01 gene
1.1	8.9	7.4	Chemokine (C-C motif) receptor-like 2
10.6	8.1	1.9	Interleukin 1 beta
1.6	8.0	1.3	P21 (CDKN1A)-activated kinase 1
9.1	7.9	1.8	Complement component 3
1.7	7.9	3.0	Upregulated during skeletal muscle growth 5
9.1	7.9	5.9	transferrin, segment 4
1.8	7.8	1.6	RIKEN cDNA B930059L03 gene
7.7	7.7	3.8	Interferon regulatory factor 5
7.1	7.7	4.3	C-type lectin domain family 4, member a3

Kid M V Kid	lung M V Lung	brain M V Brain	Gene name / Accession number
11.6	6.3	20.0	Mannose receptor, C type 1
1.2	2.4	13.3	Secreted phosphoprotein 1
10.6	17.9	12.8	Splicing factor 3b, subunit 3
10.6	3.2	11.6	F4/80
9.6	6.8	11.1	Chemokine (C-C motif) ligand 4
8.6	17.6	10.4	Lysosomal-associated protein transmembrane 5
5.6	10.2	10.4	4.5S small RNA associated ith poly-(a)-containing RNAs
7.4	3.6	9.8	Macrophage sca enger receptor 2
7.9	11.1	9.7	Fc receptor, IgG, low affinity III
10.1	5.3	9.6	Macrophage expressed gene 1
3.4	4.9	9.6	Disabled homolog 2 (Drosophila)
8.9	4.6	9.6	Lymphocyte antigen 86
8.1	5.9	9.4	Chemokine (C-C motif) ligand 2
11.0	13.5	9.2	P lysozyme structural
25.1	22.9	9.1	Dual specificity phosphatase 1
4.4	2.1	8.9	G protein-coupled receptor 34
3.0	1.7	8.8	Beta-2 microglobulin
8.6	3.7	8.8	Apolipoprotein E
11.1	21.0	8.6	Chemokine (C-X-C motif) ligand 2
1.0	9.1	8.2	S100 calcium binding protein A9 (calgranulin B)
6.1	2.0	8.2	Selenoprotein P, plasma, 1
3.4	3.9	8.1	Solute carrier family 40 (iron-regulated transporter), member 1
1.0	5.6	8.0	Chemokine (C-C motif) ligand 7
6.6	4.1	8.0	Leucine zipper, putative tumor suppressor 2
2.7	1.9	7.9	G elongation factor, mitochondrial 2
6.0	9.4	7.8	AK019039
5.4	2.8	7.6	Colony stimulating factor 1 receptor
6.9	4.4	7.5	Cathepsin S
1.1	8.9	7.4	Chemokine (C-C motif) receptor-like 2
1.0	3.8	7.4	Chemokine (C-C motif) ligand 24
3.8	2.1	7.4	Legumain
5.8	6.3	7.2	zinc finger protein 36
6.0	6.5	7.2	Protein tyrosine phosphatase, non-receptor type 18
7.9	24.3	7.1	signal-regulatory protein alpha (Sirpa)
5.1	3.7	7.1	CD53 antigen
4.8	2.8	6.9	RAS-related C3 botulinum substrate 2
8.0	12.9	6.9	FBJ osteosarcoma oncogene B
8.3	1.6	6.9	CD163 antigen
13.1	13.1	6.8	CD52 antigen
8.6	9.5	6.7	Glia maturation factor, gamma
13.2	3.6	6.7	Membrane-spanning 4-domains, subfamily A, member 6B
4.2	5.6	6.7	Complement component 1, q subcomponent, α polypeptide
0.5	7.6	6.4	Inactive X specific transcripts
11.6	4.3	6.4	Fc receptor, IgE, high affinity I, γ polypeptide
11.0	12.0	6.3	CD14 antigen
4.9	2.3	6.2	Complement component 1, q subcomponent, γ polypeptide
9.9	9.3	6.2	Chemokine (C-C motif) ligand 9
10.0	6.4	6.1	transferrin
2.5	2.7	6.0	Crystallin, beta B1
3.2	2.8	6.0	Growth arrest specific 6

Kid M V Kid	lung M V Lung	brain M V Brain	Gene name / Accession number
2.23	0.80	0.93	Solute carrier family 13 (sodium/sulphate symporters), member 1
2.23	1.46	1.21	RIKEN cDNA 2700023E23 gene
2.27	1.03	0.53	RIKEN cDNA 7330412A13 gene
2.27	0.92	0.58	Expressed sequence AI428795
2.27	1.18	1.26	PEST-containing nuclear protein
2.28	1.04	0.79	Numb
2.28	0.94	1.17	Casein kinase 1, alpha 1
2.31	0.95	0.72	Ring finger protein 14
2.33	1.00	0.63	RIKEN cDNA A730042J05 gene
2.33	0.85	0.71	Vesicle transport through interaction with t-SNAREs homolog 1A (yeast)
2.33	0.79	0.75	Aldo-keto reductase family 1, member B8
2.33	1.10	0.76	Protein tyrosine phosphatase, receptor type, D
2.33	1.14	0.88	CDNA sequence BC026657
2.35	0.59	0.80	RIKEN cDNA 9030607L02 gene
2.35	1.54	1.25	Formin binding protein 1-like
2.36	1.11	1.09	Small proline-rich protein 2F
2.38	1.86	0.79	RIKEN cDNA D230050J18 gene
2.41	0.92	0.78	AK017379
2.41	1.40	1.04	Sodium channel, nonvoltage-gated 1 gamma
2.45	1.44	0.68	Hemoglobin X, alpha-like embryonic chain in Hba complex
2.46	2.06	1.01	Claudin 10
2.50	0.98	0.83	Rap guanine nucleotide exchange factor (GEF) 5
2.53	1.02	0.94	TEA domain family member 1
2.60	0.91	0.82	RIKEN cDNA 2310057M21 gene
2.64	1.07	1.01	G protein-coupled receptor 23
2.68	1.04	0.74	SRY-box containing gene 11 (Sox11)
2.68	1.03	0.90	Tetratricopeptide repeat, ankyrin repeat and coiled-coil containing 1
2.69	0.98	0.72	RIKEN cDNA 2310007 11 gene
2.71	0.69	0.71	ST6 (alpha-N-acetyl-neuraminyl-2,3-beta-galactosyl-1,3)-N-acetylgalactosaminide alpha-2,6-sialyltransferase 3
2.71	1.01	1.33	Thiopurine methyltransferase
2.75	0.79	0.47	RIKEN cDNA 3110001N23 gene
2.75	1.08	0.89	RIKEN cDNA 9430072K23 gene
2.77	0.88	1.02	RIKEN cDNA 2310005E10 gene
2.77	1.01	1.14	GATA binding protein 3
2.81	1.11	0.49	Tripartite motif-containing 35
2.91	1.17	1.00	RIKEN cDNA 2310004K06 gene
2.93	0.98	0.86	AK014078
2.97	1.96	0.94	Protein kinase C, nu
3.10	1.13	1.08	Zinc finger protein 553
3.18	1.59	0.53	Hemoglobin Z, beta-like embryonic chain
3.23	0.79	1.11	RIKEN cDNA 4122401K19 gene
3.34	0.81	0.57	RIKEN cDNA 9030411K21 gene
3.36	1.08	0.84	RIKEN cDNA 5830428H23
3.39	1.61	1.23	Suppression of tumorigenicity 13
3.46	1.00	1.00	Gap junction membrane channel protein beta 4
3.76	0.79	0.67	RIKEN cDNA 2900056M20 gene
3.84	1.19	1.27	Secreted frizzled-related sequence protein 1
3.94	0.93	1.02	AK007529
4.50	0.90	1.41	Homeo box D4
6.63	1.28	1.40	Stress 70 protein chaperone, microsome-associated, human homolog

The macrophage-enriched genes with the highest fold change from kidney, brain and lung macrophages are listed in columns 1, 2 and 3, respectively. A visual comparison of columns 1–3 illustrates the high degree of concordance between the gene expression of resident macrophages in all tissues (columns 1–3). In contrast, the genes showing enrichment in the kidney as tissue of origin (column 4) show no concordance with those enriched in lung and brain. Red indicates higher relative expression in macrophages. Green demonstrates higher relative expression in host tissue. Genes common to 2/3 lists are highlighted in pale yellow. Genes common to all three lists are shown in bright yellow. UGI name is listed for each gene where available. If there is no gene name, an accession number is listed.

Table 2
A comparison of the genes demonstrating the highest *B*-score change between macrophage and tissue of origin, indicating those gene for which there is the highest statistical confidence of an enrichment in one population versus another

Kid M V Kid	lung M V Lung	brain M V Brain	Gene name / Accession number
9.12	3.43	3.36	transferrin
9.09	4.10	4.70	Mannose receptor, C type 1
8.79	3.49	3.71	CD52 antigen
8.64	2.30	6.21	Apolipoprotein E
8.61	2.85	6.65	Chemokine (C-X-C motif) ligand 2
8.61	2.83	4.75	Lysosomal-associated protein transmembrane 5
8.60	2.41	3.85	transferrin, segment 4
8.55	3.49	3.59	S100 calcium binding protein A8 (calgranulin A)
8.51	2.48	3.81	P lysozyme structural
8.47	2.27	2.04	Macrophage expressed gene 1
8.39	2.41	4.08	Lymphocyte antigen 86
8.26	0.69	6.04	triggering receptor expressed on myeloid cells 2
8.15	3.53	0.25	Pleckstrin homol., Sec7 & coiled-coil domains, binding prot.
7.92	2.63	2.02	FBJ osteosarcoma oncogene B
7.91	1.42	5.19	Zinc finger protein 36
7.86	-0.49	3.02	Solute carrier family 11, member 1
7.83	2.75	-0.27	Arachidonate 5-lipoxygenase activating protein
7.79	3.65	6.67	Leucine zipper, putative tumor suppressor 2
7.72	-7.29	-6.51	T-box 20
7.65	3.90	4.09	Protein tyrosine phosphatase, non-receptor type 18
7.63	3.84	1.66	Fc receptor, IgE, high affinity I, gamma polypeptide
7.61	3.18	2.46	Lysozyme
7.60	0.55	-0.65	Allograft inflammatory factor 1
7.58	3.13	2.89	C-type lectin domain family 7, member a
7.57	3.03	6.69	Legumain
7.51	2.66	5.32	Complement component 1, q subcomponent, γ polypeptide
7.50	1.70	0.03	Adipose differentiation related protein
7.47	1.68	6.26	Growth arrest specific 6
7.43	2.39	2.19	B-cell translocation gene 2, anti-proliferative
7.42	3.05	6.50	Cathepsin S
7.38	0.44	2.55	Coronin, actin binding protein 1A
7.32	3.83	3.63	Spermidine/spermine N1-acetyl transferase 1
7.31	2.36	-0.10	B-cell leukemia/lymphoma 2 related protein A1c
7.26	1.60	3.85	Fc receptor, IgG, high affinity I
7.25	-6.74	3.93	AK020996
7.17	2.06	1.23	CD68 antigen
7.16	-5.76	3.16	NM_028084
7.10	3.12	2.73	Chemokine (C-C motif) ligand 2
7.10	-2.16	-4.52	Activating transcription factor 6
7.08	-4.33	2.92	Early growth response 2
7.04	1.79	6.91	Fc receptor, IgG, low affinity III
7.04	1.94	2.25	Scavenger receptor class B, member 2
7.03	-2.03	-4.25	Eukaryotic translation elongation factor 2
6.98	3.27	3.84	Docking protein 2
6.97	3.72	6.64	Colony stimulating factor 1 receptor
6.88	2.05	6.10	RAS-related C3 botulinum substrate 2
6.88	0.59	6.03	4.5S small RNA associated with poly-(a)-containing RNAs
6.87	0.23	-1.86	Phorbol-12-myristate-13-acetate-induced protein 1
6.87	-0.30	3.24	Selenoprotein P, plasma, 1
6.86	3.95	1.22	Interleukin 1 beta

Kid M V Kid	lung M V Lung	brain M V Brain	Gene name / Accession number
2.79	5.74	1.44	Leukocyte Ig-like receptor, subfamily B, member 4 (Gp49a)
-7.62	5.57	4.62	Chemokine (C-C motif) receptor-like 2
3.58	5.54	3.24	U3B small nuclear RNA 4
-3.89	5.29	-1.66	Cytochrome P450, family 2, subfamily j, polypeptide 9
-0.91	5.09	3.23	X56974
5.98	5.07	3.47	Interferon regulatory factor 5
-3.63	5.02	-1.21	Thioredoxin domain containing 4 (endoplasmic reticulum)
6.04	4.99	6.03	Chemokine (C-C motif) ligand 4
3.47	4.99	0.99	NADH dehydrogenase chain 5
-7.63	4.85	2.05	S100 calcium binding protein A9 (calgranulin B)
-1.90	4.83	1.91	X81439
6.25	4.77	1.24	Inositol polyphosphate-5-phosphatase D
-5.01	4.68	-0.43	Homeo box B7
3.40	4.66	-4.21	AK021211
2.69	4.49	-0.91	Eukaryotic translation initiation factor 4E member 3
1.45	4.38	4.14	Metallothionein 1
4.13	4.37	3.98	Interferon activated gene 203
4.23	4.31	3.48	G-protein coupled receptor 65
1.06	4.29	-2.92	Membrane-associated ring finger (C3HC4) 7
6.31	4.21	-0.73	Complement component 3a receptor 1
9.09	4.10	4.70	Mannose receptor, C type 1
4.34	4.06	-2.70	B-cell leukemia/lymphoma 2 related protein A1b
2.10	3.98	-2.95	Leukotriene B4 receptor 1
2.14	3.97	1.13	AK003694
3.69	3.97	5.87	triggering receptor expressed on myeloid cells 2 (Trem2)
6.86	3.95	1.22	Interleukin 1 beta
5.42	3.92	6.14	Membrane-spanning 4-domains, subfamily A, member 6B
7.65	3.90	4.09	Protein tyrosine phosphatase, non-receptor type 18
5.00	3.90	-1.00	S100 calcium binding protein A4
-2.13	3.87	4.19	AHNAK nucleoprotein (desmoyokin)
6.30	3.87	6.28	CD14 antigen
4.14	3.85	-0.35	Telomerase associated protein 1
3.90	3.84	2.44	S100 calcium binding protein A13
7.63	3.84	1.66	Fc receptor, IgE, high affinity I, gamma polypeptide
4.40	3.84	-0.83	Membrane-spanning 4-domains, subfamily A, member 6C
7.32	3.83	3.63	Spermidine/spermine N1-acetyl transferase 1
2.05	3.83	3.99	Proviral integration site 1
6.54	3.82	3.65	Chemokine (C-C motif) ligand 12
0.13	3.76	1.09	SFFV proviral integration 1
-0.27	3.76	-1.06	RIKEN cDNA 2810449M09 gene
-4.88	3.76	3.86	TEF-1-related factor (FR-19)
6.97	3.72	6.64	Colony stimulating factor 1 receptor
6.18	3.70	6.29	Disabled homolog 2 (Drosophila)
-3.38	3.68	-3.46	RIKEN cDNA 1600014K23 gene
-7.83	3.68	-4.36	RIKEN cDNA C030002B11 gene
3.68	3.67	1.29	B-cell leukemia/lymphoma 2 related protein A1d
-3.20	3.67	-4.20	HemK methyltransferase family member 1
-6.57	3.67	-1.26	Immunoglobulin kappa chain variable 21 (V21)
7.79	3.65	6.67	Leucine zipper, putative tumor suppressor 2
-1.81	3.63	-5.22	Immunoglobulin heavy chain 6 (heavy chain of IgM)

Kid M V Kid	lung M V Lung	brain M V Brain	Gene name / Accession number
7.04	1.79	6.91	Fc receptor, IgG, low affinity III
5.15	3.52	6.77	F4/80
7.57	3.03	6.69	Legumain
7.79	3.65	6.67	Leucine zipper, putative tumor suppressor 2
8.61	2.85	6.65	Chemokine (C-X-C motif) ligand 2
6.97	3.72	6.64	Colony stimulating factor 1 receptor
-1.37	2.77	6.59	Secreted phosphoprotein 1
7.42	3.05	6.50	Cathepsin S
2.22	0.95	6.50	Beta-2 microglobulin
6.60	2.64	6.39	Dual specificity phosphatase 1
1.80	0.73	6.38	G protein-coupled receptor 34
6.18	3.70	6.29	Disabled homolog 2 (Drosophila)
6.30	3.87	6.28	CD14 antigen
7.47	1.68	6.26	Growth arrest specific 6
5.91	2.22	6.23	Splicing factor 3b, subunit 3
8.64	2.30	6.21	Apolipoprotein E
3.18	1.68	6.19	Inactive X specific transcripts
5.42	3.92	6.14	Membrane-spanning 4-domains, subfamily A, member 6B
6.88	2.05	6.10	RAS-related C3 botulinum substrate 2
6.01	-0.29	6.09	RIKEN cDNA C030027H14 gene
8.26	0.69	6.04	triggering receptor expressed on myeloid cells 2 (Trem2)
6.04	4.99	6.03	Chemokine (C-C motif) ligand 4
6.88	0.59	6.03	4.5S small RNA associated with poly-(a)-containing RNAs
3.72	2.41	5.99	Gem-interacting protein
2.00	1.47	5.95	Pleckstrin homology, Sec7 and coiled/coil domains 4
1.67	2.88	5.94	Crystallin, beta B1
2.33	-0.30	5.90	BC005512
3.69	3.97	5.87	triggering receptor expressed on myeloid cells 2 (Trem2)
5.29	-2.47	5.86	Membrane-spanning 4-domains, subfamily A, member 7
6.21	-4.24	5.80	Protective protein for beta-galactosidase
2.67	-6.80	5.69	Ficolin A
3.00	1.88	5.69	Chromatin modifying protein 4B
6.41	1.57	5.66	Anti-Mullerian hormone
2.37	0.74	5.62	Tumor necrosis factor receptor superfamily, member 1a
5.39	3.26	5.62	Glycine amidinotransferase
2.75	-2.49	5.61	Caspase 8
4.27	-2.18	5.56	Macrophage scavenger receptor 2
2.55	1.31	5.50	Epstein-Barr virus induced gene 3
5.35	-1.88	5.49	Cysteine-rich secretory protein 3
3.90	-2.60	5.49	RIKEN cDNA 4833414E09 gene
5.14	-0.75	5.44	Immunoglobulin heavy chain 6 (heavy chain of IgM)
4.03	-0.19	5.41	Talin 1
0.99	1.62	5.38	RIKEN cDNA 2210010B09 gene
7.51	2.66	5.32	Complement component 1, q subcomponent, γ polypeptide
4.55	-3.97	5.26	Paraoxonase 3
4.74	-1.93	5.25	Spinocerebellar ataxia 2 homolog (human)
6.47	2.05	5.25	TYRO protein tyrosine kinase binding protein
7.91	1.42	5.19	Zinc finger protein 36
-2.59	-0.70	5.14	UDP glucuronosyltransferase 1 family, polypeptide A6
-2.49	-4.13	5.14	Chemokine-like factor super family 3

The macrophage-enriched genes with the highest *B*-score from kidney, brain and lung macrophages are listed in columns 1, 2 and 3, respectively. A visual comparison of columns 1–3 illustrates the high degree of concordance between resident macrophages in all tissues. Red indicates higher confidence of enrichment in macrophages. Green demonstrates higher confidence of enrichment in host tissue. Genes common to 2/3 lists are highlighted in pale yellow. Genes common to all three lists are shown in bright yellow.

The results of this profiling showed that many well characterised macrophage-specific and macrophage-associated genes were represented amongst the outliers for the EGFP-enriched macrophage populations. This included the macrophage transcription factor, PU.1 (sfpi1), the F4/80 antigen (EMR1), and lysozyme, all shown to have similar distributions to *Csf1r* in whole mount *in situ* hybridization profiles (Lichanska et al., 1999). Other macrophage genes expressed include chemokine (C–C) and (C–X–C) ligands (including CXCL1, CXCL2, CCL2, CCL4, CCL6, CCL7, CCL9, CCL12, CCL24) and receptors (including CX3CR1, which was previously used a marker for yolk-sac-derived macrophages), as well as many membrane receptors that are commonly used as definitive macrophage markers (sialoadhesin, Mac1, F4/80 (EMR-1, EGF-like module containing, mucin-like, hormone receptor-like sequence)). By extension, the significant numbers of unannotated genes on these lists are likely to be macrophage functional genes. Section RNA *in situ* hybridization was performed on >20 genes with enriched expression in renal macrophages. The expression patterns depicted in Fig. 4 validate both the isolation and profiling data. *Csf1r* was detected by RNA *in situ* hybridization suggested an expressing

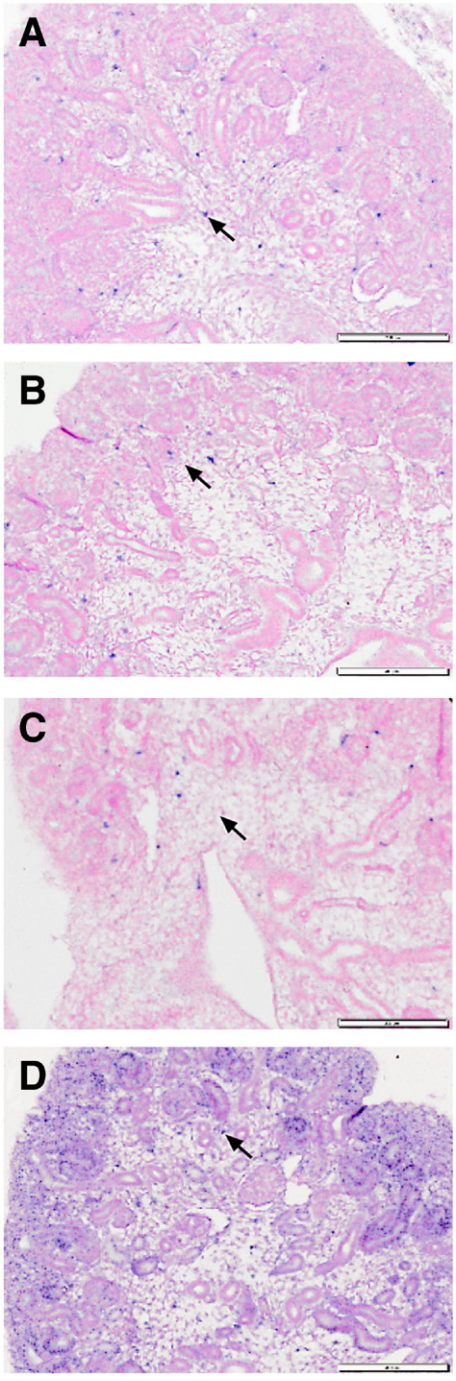

Fig. 4. Localization of genes enriched in kidney macrophages. RNA *in situ* hybridisation of E15.5 kidneys showed expression in the medullary regions for (A) *Csf1r* (*c-fms*) and (B) macrophage scavenger receptor 1 (Msr1), whereas (C) Glycoprotein 49B (Gp49b) possibly marked a smaller subset of macrophages located at the corticomedullary junction of the kidney. (D) Lysosomal-associated protein transmembrane 5 (Laptm5) was not exclusively expressed in macrophages. Punctate expression was also seen in tubules, glomeruli and interstitium. Scale bar = 100 μm.

population consistent with the 2–5% indicated following FACS analysis (Fig. 4A). Macrophage scavenger receptor 1 (Msr1) marked an apparently identical population of macrophages (Fig. 4b). Glycoprotein 49B (Gp49b) appeared to mark a smaller subset of macrophages at the corticomedullary junction of the kidney (Fig. 4c). Such subpopulations may represent different types of cells or different stages of monocytic maturation, as has been shown previously during in mouse embryos for markers such as F4/80 which first appears later in development than csf1r (Lichanska et al., 1999).

Effects of CSF-1 in kidney explant culture and changes in gene expression

The traditional view of macrophage function in the embryo is phagocytic clearance of dying cells (Henson and Hume, 2006). In contrast, a trophic role has been implied in many adult tissues undergoing regeneration (Pull et al., 2005). In a recent study of the role of macrophages in pancreatic development in mice, Geutskens et al. (2005) noted that their numbers continued to increase in organ culture, suggesting an autonomous proliferative activity, and that they could be expanded further with *ex vivo* treatment of organ cultures with CSF-1. We therefore asked whether CSF-1 could increase macrophage numbers in the kidney, and whether there would be a consequential modulation of renal development. 100 U/μl human recombinant CSF-1 was added to kidney explant culture to determine its effects on branching and nephron formation. The effects of CSF-1 alone as a stimulus were inconsistent across experiments. We considered the possibility that there is an endogenous ligand that acts in concert with CSF-1, by analogy with RANKL in the differentiation of osteoclasts (Blair et al., 2005) and our data showing that CSF-1 acts in concert with lipopolysaccharide (LPS) (Sweet et al., 2002). LPS alone had no effect on differentiation of explanted kidneys; however, addition of low concentrations of LPS permitted a consistent response to CSF-1. Development was assessed by immunofluorescence for calbindin 28 kDa and WT1 to highlight the development of the branching ureteric tree and developing nephrons respectively (Fig. 5A). Addition of CSF-1 to explanted 11.5–12.0 dpc kidneys resulted in a statistically significant increase in the number of branch tips and nephrons after 4 days in culture (Fig. 5B).

To identify the molecular changes that occur after the addition of CSF-1, expression profiling was performed on CSF-1-treated explants compared with untreated explants. The 50 highest ranked genes based on a fold-change and B-statistic are shown in Table 3. Seventeen of the top 20 outliers upregulated (based on fold-change) in CSF-1-treated explants were also found to be upregulated (based on fold change) in the resident renal macrophage list, indicating that CSF-1 specifically upregulates macrophage genes, most likely by increasing the number of macrophages present during culture. 11.5 dpc explants from *Csf1r–ECFP* mice were cultured with or without the addition of CSF-1 (Figs. 5Ai, j), the increased apparent abundance of ECFP-positive cells confirming an increase in the macrophage population in the CSF-1-treated explants. The upregulation of calbindin 28 kDa, which is encoded specifically by the developing ureteric tree, shows a disproportionate increase in tree branching, suggesting that the primary event is a stimulation of ureteric branching followed by an increase in formation of nephron condensates.

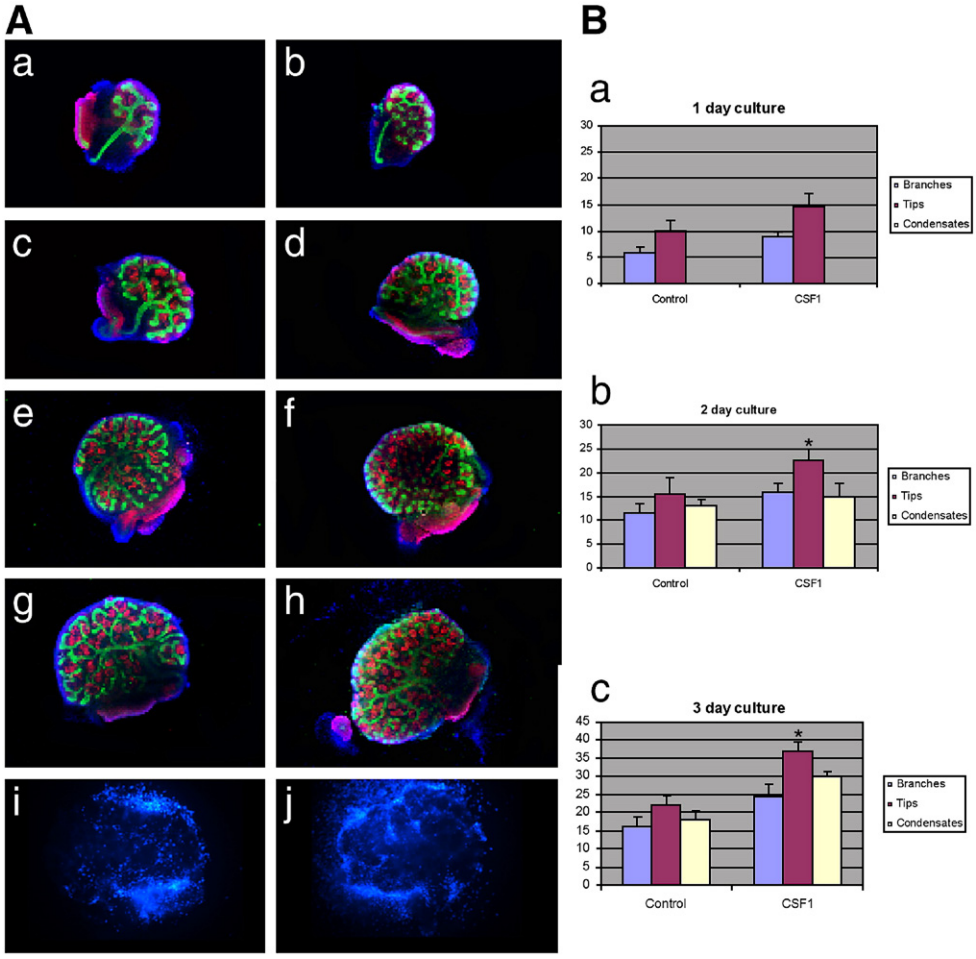

Fig. 5. (A) Metanephric explant culture of 11.5 dpc kidneys cultured with CSF-1 (100 U/ml)+LPS (0.1 ng/ml) (b, d, f, h, j) or LPS alone (control; a, c, e, g, i) explants. Explants were cultured for 1 (a, b), 2 (c, d), 3 (e, f), 4 (g, h) or 5 days (i, j). In panels a–h wild-type mice were used and immunofluorescence was performed to reveal the ureteric tree (calbindin-D28K, green), forming nephrons (WT1, red) and all nuclei (DAPI, blue). In panels i and j, *Csf1r–ECFP* mice were used and the blue fluorescence show the CFP-positive macrophages present in the cultures. (B) Total numbers of ureteric tree branches, ureteric tips and condensates in control versus CSF-1-treated explants at 1 day (a), 2 days (b) and 3 days (c) of culture. Error bars represent the standard deviation of the mean for one representative experiments. Experiments were performed at least twice for each time point. Asterisks indicate where there is a significant different ($p<0.05$) between control and CSF-1-treated explants.

A number of genes upregulated in explants in response to CSF-1 were predicted to encode secreted proteins, including chemokines. We investigated whether these chemokines were responsible, alone or in combination, for some of the trophic roles of CSF-1. Unlike CSF-1, the addition of recombinant CCL9, CCL4, CCL4+CCL9, CCL6, Cxcl1 or Gas6 showed no visible or significant effect on kidney explant development (data not shown).

An analysis of the genes marking embryonic macrophages in general and also genes induced in response to culture of explants in CSF-1 showed a link with the alternate or M2 pathway of macrophage activation. The alternate activation pathways have been implicated in an anti-inflammatory, pro-proliferative role for macrophages. A modified version of the M2 response occurs in tumour-associated macrophages (Mantovani et al., 2004), suggesting that this may be important for the trophic role played by macrophages in tumours. The M2 pathway is classically induced in response to IL-4 and IL-3 and results in the upregulation of IL-10 and TGFβ (Mantovani et al., 2004; Sica et al., 2006). While these genes were not overrepresented in embryonic macrophages or upregulated in response to CSF-1, a number of M2-associated genes identified in tumour-associated macrophages were present on embryonic macrophages, including macrophage mannose receptor, macrophage scavenger receptors 1 and 2 (*Msr1*, *Msr2*), *CCL24* and *C1q*. Van Ginderachter et al. (2006) suggest that the M2 response *ex vivo* during different pathologies is characterised by the expression of genes linked to wound healing and angiogenesis, including *selenoprotein P* and *TREM2*. Both of these genes were enriched in resident embryonic macrophages and Trem2 was strongly induced in explants in response to CSF-1 (see Tables 1–3 and http://kidney.scgap.org/CSF1_Supp_Data/Macrophage_summary/Supp_table1.xls). Trem2 appears to attenuate the production of cytokines associated with classical activation (Turnbull et al., 2006). A more recent analysis of the transcriptome of human monocytes during differentiation and polarization highlighted a set of genes differentially expressed in M2 macrophages (Martinez et al.,

Table 3
Genes induced in embryonic kidney explants in response to the addition of CSF-1, as assessed by fold change and B-statistic

Fold X	B	Gene Name	Accession number	UGI number	Fold X	B	Gene Name	Accession number	UGI number
2.9	6.64	minichromosome maintenance deficient domain containing 1	AK018494	Mm.278221	4.8	2.97	chemokine (C-C motif) ligand 9	NM_011338	Mm.2271
2.3	6.48	myeloid leukemia factor 2	BC003975	Mm.29737	4.4	3.22	secreted phosphoprotein 1	NM_009263	Mm.288474
2.3	6.44	triggering receptor expressed on myeloid cells 2	NM_031254	Mm.261623	4.3	1.89	chemokine (C-C motif) ligand 4	NM_013652	Mm.244263
2.5	6.39	actin related protein 2/3 complex, subunit 1B	AF162768	Mm.30010	3.9	2.98	glycoprotein 49 B	NM_013532	Mm.34408
2.9	6.35	FXYD domain-containing ion transport regulator 5	NM_008761	Mm.1870	3.7	2.42	Fc receptor, IgG, low affinity IIb	NM_010188	Mm.22119
2.3	6.24	short coiled-coil protein	AK010984	Mm.352239	3.7	2.00	Fc receptor, IgE, high affinity I, gamma polypeptide	NM_010185	Mm.22673
2.9	6.15	glyceraldehyde-3-phosphate dehydrogenase homolog	AK013857		3.6	2.38	macrophage expressed gene 1	L20315	Mm.3999
2.1	6.10	scinderin	NM_009132	Mm.2416	3.6	1.88	B-cell leukemia/lymphoma 2 related protein A1a	NM_009742	Mm.425593
3.3	5.80	CD68 antigen	NM_009853	Mm.15819	3.5	3.36	B-cell leukemia/lymphoma 2 related protein A1d	NM_007536	Mm.378888
3.4	5.77	complement component 1, q subcomponent, γ polypeptide	NM_007574	Mm.2570	3.5	4.46	lysozyme	NM_017372	Mm.45436
2.8	5.61	capping protein (actin filament), gelsolin-like	NM_007599	Mm.18626	3.5	3.21	P lysozyme structural	NM_013590	Mm.177539
2.0	5.60	microfibrillar-associated protein 2	NM_008546	Mm.7386	3.4	5.77	complement component 1, q subcomponent, γ polypeptide	NM_007574	Mm.2570
1.9	5.58	proteasome (prosome, macropain) inhibitor subunit 1	BC012260	Mm.146984	3.3	5.80	CD68 antigen	NM_009853	Mm.15819
2.0	5.58	legumain	NM_011175	Mm.17185	3.2	2.45	Arachidonate 5-lipoxygenase activating protein	M96554	Mm.19844
3.0	5.57	Fc receptor, IgG, low affinity IIb	NM_010187	Mm.425062	3.1	4.60	calbindin-28K	NM_009788	Mm.277665
2.4	5.51	triggering receptor expressed on myeloid cells 2	NM_031253		3.0	5.57	Fc receptor, IgG, low affinity IIb	NM_010187	Mm.425062
1.9	5.43	transmembrane protein 9	NM_025439	Mm.41773	3.0	1.90	Membrane-spanning 4-domains, subfamily A, member 6D	NM_026835	Mm.290390
2.4	5.32	small chemokine (C-C motif) ligand 11	NM_011330	Mm.4686	2.9	1.77	annexin A3	NM_013470	Mm.7214
1.9	5.32	apolipoprotein E	NM_009696	Mm.305152	2.9	6.15	glyceraldehyde-3-phosphate dehydrogenase homolog	AK013857	
1.7	5.32	melanocyte proliferating gene 1	NM_021713		2.9	2.77	F4/80	U66888	Mm.2254
1.9	5.26	protein tyrosine phosphatase, non-receptor type 18	NM_011206	Mm.361	2.9	2.17	cyclin-dependent kinase 4	NM_009870	Mm.6839
1.9	5.22	histocompatibility 2, Q region locus 1	X65748	Mm.195061	2.9	6.64	minichromosome maintenance deficient domain containing 1	AK018494	Mm.278221
1.9	5.04	RIKEN cDNA 0610007P14 gene	NM_021446	Mm.143795	2.9	6.35	FXYD domain-containing ion transport regulator 5	NM_008761	Mm.1870
1.8	4.98	mannose phosphate isomerase 1	AF244360	Mm.247218	2.9	4.18	ficolin A	NM_007995	Mm.10510
2.7	4.89	UDP glucuronosyltransferase 2 family, polypeptideB37	NM_053215	Mm.160362	2.8	5.61	capping protein (actin filament), gelsolin-like	NM_007599	Mm.18626
2.2	4.86	serologically defined breast cancer antigen 84	NM_025516	Mm.141276	2.8	3.80	CD14 antigen	NM_009841	Mm.3460
2.1	4.85	peripheral myelin protein	NM_008885	Mm.1237	2.8	1.95	CD52 antigen	M55561	Mm.24130
1.6	4.84	Inactive X specific transcripts	L04961	Mm.274770	2.7	4.89	UDP glucuronosyltransferase 2 family, polypeptideB37	NM_053215	Mm.160362
1.6	4.83	deleted in polyposis 1-like 1	AB039933	Mm.28147	2.6	2.83	mitogen activated protein kinase kinase 4	U18310	Mm.27491
1.6	4.79	Ywhaq	NM_011739	Mm.289630	2.6	0.87	regulator of G-protein signaling 1	NM_015811	Mm.103701
1.6	4.75	death-associated protein	BC010828	Mm.222867	2.5	1.71	mannose-P-dolichol utilization defect 1	NM_011900	Mm.89579
1.5	4.75	succinate-Coenzyme A ligase, GDP-forming, beta subunit	AF058956	Mm.371585	2.5	2.33	lectin, galactose binding, soluble 9	NM_010708	Mm.341434
1.6	4.69	histocompatibility 2, class II antigen A, beta 1	NM_010379		2.5	6.39	actin related protein 2/3 complex, subunit 1B	AF162768	Mm.30010
1.6	4.66	Transmembrane emp24 protein transport domain containing 9	NM_026211	Mm.45233	2.5	3.04	Reticulocalbin 3, EF-hand calcium binding domain	BC005487	Mm.29997
1.5	4.62	immunoglobulin kappa chain variable 1 (V1)	M23421	Mm.423468	2.5	1.91	B-cell leukemia/lymphoma 2 related protein A1c	NM_007535	Mm.378887
3.1	4.60	calbindin-28K	NM_009788	Mm.277665	2.5	0.95	dehydrogenase/reductase (SDR family) member 1	NM_026819	Mm.21623
2.3	4.56	TYRO protein tyrosine kinase binding protein	NM_011662	Mm.46301	2.4	4.28	muscle and microspikes RAS	NM_008624	Mm.2045
1.8	4.52	Zinc finger, MYM domain containing 1	NM_026670	Mm.273806	2.4	1.24	glyceraldehyde-3-phosphate dehydrogenase	NM_008084	Mm.343110
1.5	4.52	chemokine (C-X-C motif) ligand 11	NM_019494		2.4	5.51	triggering receptor expressed on myeloid cells 2	NM_031253	
1.5	4.49	actinin alpha 4	U41416	Mm.276042	2.4	3.82	cathepsin S	NM_021281	Mm.3619
1.5	4.49	small nuclear ribonucleoprotein polypeptide A	NM_015782	Mm.386890	2.4	3.26	lysosomal-associated protein transmembrane 5	NM_010686	Mm.271868
1.6	4.48	RIKEN cDNA 1700037H04 gene	NM_026091	Mm.27711	2.4	1.14	Similar to hypothetical protein FLJ38281	AK020201	Mm.148033
3.5	4.46	lysozyme	NM_017372	Mm.45436	2.4	0.79	complement component 1, q subcomponent, α polypeptide	NM_007572	Mm.2570
1.5	4.42	RIKEN cDNA 0610011I04 gene	BC010831	Mm.27061	2.4	5.32	small chemokine (C-C motif) ligand 11	NM_011330	Mm.4686
1.5	4.39	activating transcription factor 3	NM_007498	Mm.2706	2.4	1.96	C-type lectin, superfamily member 8	NM_010819	Mm.271782
2.3	4.37	glycoprotein (transmembrane) nmb	AJ251685	Mm.302602	2.3	6.44	triggering receptor expressed on myeloid cells 2 (Trem2)	NM_031254	Mm.261623
1.5	4.37	tubulin, gamma 1	BC006581	Mm.142348	2.3	6.24	short coiled-coil protein	AK010984	Mm.352239
1.6	4.33	T cell receptor, V-J alpha junctional region (clone T1CRP28)	Z86029	Mm.429462	2.3	6.48	myeloid leukemia factor 2	BC003975	Mm.29737
1.7	4.33	aortic preferentially expressed gene 1	NM_007463	Mm.275397	2.3	3.25	PCTAIRE-motif protein kinase 3	NM_008795	Mm.28130
2.2	4.32	prostaglandin D2 synthase 2, hematopoietic	NM_019455	Mm.143720	2.3	4.24	Transmembrane protein 97	X81718	Mm.29431

The top 50 genes enriched in explants in response to CSF-1 treatment are depicted based on fold change (right) and *B*-score (left). Yellow shading indicates those genes overlapping with the macrophage enriched genes in Tables 1 and 2.

2006). This included *CD36*, *cathepsin C* and *selenoprotein P1*, which are all strongly expressed in GFP-positive cells from all three organs examined.

Discussion

This study provides the first comprehensive overview of the infiltration of the developing embryo by macrophages detected with a convenient EGFP reporter gene, examines their molecular phenotype, and sheds light on their possible function in kidney development.

The majority of the literature on macrophages in embryonic development focuses on their role in removal of apoptotic cell bodies. This is certainly a major activity, and one that is conserved from *Drosophila* through to mammals (Henson and Hume, 2006). Several receptors are likely to be involved in this recognition process, including abca1 (conserved from *Drosophila*), the macrophage scavenger receptor, the phosphatidyl serine receptor and CD36. All of these genes, and many others (macrophage mannose receptor, *C1q*, *Msr2*, *galectin 1*, *galectin 3*, *galectin 9*, *SRB2*, *C1q*, C type lectins *Clec4a2*, *4a3*, *7a*, *4n*, *Gas6*), as well as several lysosomal hydrolases and lysosome-associated proteins (LAMPs, CD68) were enriched in the *Csf1r–EGFP*-positive embryonic macrophages (Tables 1 and 2). This extensive repertoire may explain why the knockout of individual receptors does not appear to impair the removal of dead cells. In fact, in at least some sites in the body, the removal of apoptotic cells can be carried out by “facultative” phagocytes (neighbouring mesenchymal cells) in animals that lack normal macrophage populations due to mutation in the *PU.1* gene

(Wood et al., 2000). These animals are not deficient in yolk-sac-derived macrophages, which might provide some essential phagocyte functions (Lichanska et al., 1999).

The trophic function of macrophages is implied from the substantive growth deficiency in animals that have mutations in either CSF-1, or the CSF-1 receptor (Dai et al., 2002). In addition to global growth defects, some organs that are especially affected include bone, the sensory nervous system, gonads, mammary gland and pancreas (Banaei-Bouchareb et al., 2004; Cohen et al., 1996; Michaelson et al., 1996; Van Nguyen and Pollard, 2002). These developmental abnormalities may reflect a physiological role for CSF-1 itself, since the levels of CSF-1 mRNA and protein increase with gestational age and exhibit a postnatal spike (Roth and Stanley, 1996). The absence in CSF-1-deficient mice of definitive loss of function or apparent structural disturbance in other organs should not be taken as evidence that the macrophage role is dispensable. Macrophages detected using the F4/80 marker (which is itself CSF-1-sensitive; Carninci et al., 2006; Hume et al., 1988) (see also www.macrophages.com) are not completely depleted in any organ of the *CSF-1* or *Csf1r*-deficient mouse lines. In the former case, CSF-1 may be derived from the maternal circulation if the mother is heterozygous (Roth et al., 1998). The effect of the *Csf1r* mutation is more penetrant, presumably because it cannot be overcome by CSF-1 from the mother (Dai et al., 2002).

Monocytes that tune inflammatory responses, scavenge debris, promote angiogenesis and tissue remodelling and repair have been referred to as M2 macrophages (Gordon and Taylor, 2005; Mantovani et al., 2004; Wilson et al., 2004), extending a rather imperfect analogy with the Th_1/Th_2 helper T cell dichotomy. The macrophages found within tumours probably constitute a novel subclass of these so-called M2 macrophages (Biswas et al., 2006; Mantovani et al., 2005; Sica et al., 2006). The phenotype of the embryonic macrophages characterised herein overlaps with the published tumor-associated macrophage data, in particular overlapping the chemokine (e.g. CCL2) and receptor (galectin 1, scavenger receptor A, msr2, C1q, mannose receptor) markers highlighted by others (Mantovani et al., 2004). This phenotype in tumour-associated macrophages has recently led to a novel approach to cancer therapy, involving immunisation against legumain, the lysosomal asparaginyl endopeptidase (Luo et al., 2006), which is also enriched in embryonic macrophages. Taken together, the data suggest that there are significant similarities between the foetal and tumour environments that lead to common macrophage phenotype. By extension, the macrophages in the tumours and embryos are likely to share trophic mechanisms, and an understanding of the roles of macrophages in embryogenesis may be translated into therapeutic applications in malignancy.

In the current study, we have added the kidney to the list of organs whose growth is positively affected by resident embryonic macrophages. The addition of CSF-1 to explanted developing kidneys elicited a remarkable increase in rate of development. There are several ways by which CSF-1 may generate a trophic effect on the developing kidney. The first is the possibility that the macrophages respond to CSF-1 signaling via the production of one or more critical factors that enhance renal development. These may involve secreted factors or a growth signal mediated by surface tethered or transmembrane proteins able to signal to adjacent renal cells. The ability of several individual chemokines to mimic CSF-1 was eliminated, but a complex milieu may be required. The second possibility is a net increase in the clearance of apoptotic cells due to stimulation of the macrophages. The profiling of explants± CSF-1 did not reveal significant changes in apoptotic markers that would support this. The third option is that CSF-1, simply by increasing the number of resident macrophages, enhances the proliferative milieu being provided by these cells. The similarity between the profile of resident macrophages and tumour-associated macrophages would support this concept. Finally, there might be direct signalling by CSF-1 to another cell population within the kidney. This possibility is supported by the relatively low apparent enrichment for *Csf1r* expression that was seen when comparing embryonic macrophages with their resident tissue. While *in situ* hybridization and analysis of the *Csf1r* transgenics themselves did not suggest the existence of any other *Csf1r*-positive cells, it is possible that there is widespread low levels of *Csf1r* expression throughout the kidney which may transduce the CSF-1 response. However, our observations of an intimate relationship between the resident renal macrophage and the developing renal tubules, coupled with the observed response of the developing kidney to CSF-1, suggests a niche-like relationship between macrophage and tubule that may be critical for repair. Indeed, the major sites of CSF-1 production within the damaged kidney are the tubular epithelial cells themselves (Isbel et al., 2001). A similar niche has been recently shown for the resident macrophage in the colonic crypts (Pull et al., 2005).

An analysis of the secreted proteins being produced by embryonic macrophages reveals many C–C and CXC motif chemokine ligands known to play roles in directed migration, activation and proliferation. The expression of receptors for Ccl and Cxcl chemokines on renal cells, including podocytes and collecting duct cells (Le Meur et al., 2004), suggests that these ligands can signal to the kidney itself rather than simply playing a role in monocyte attraction. Transferrin is a major plasma iron-completing protein made by peritoneal macrophages and the liver that transports ferric iron to all tissues (Yang et al., 1990). Its presence within serum-free culture media has long been shown to be essential for organ culture (Avner et al., 1985; Ekblom and Thesleff, 1985). In combination with insulin, transferrin enhances cell proliferation in cultures of human fetal kidney (Briere et al., 1991) and potentiates the activity of EGF on mitogenesis (Chailler et al., 1991). The source of renal transferrin *ex vivo* has not previously been investigated. Our data show that one source of renal transferrin is the resident macrophage.

The existence of monocyte-derived cells within the adult kidney has recently been reported using a CX3CR1-transgenic line. These cells were referred to as dendritic cells (DCs) and suggested to play an immune sentinel role in the post-natal kidney (Soos et al., 2006). As noted previously, CX3CR1 is also a marker of yolk-sac-derived phagocytes (Bertrand et al., 2005b). In concordance with our data, the network of CX3CR1-

positive cells within the kidney lay within the interstitium with close proximity to the tubular cells (Soos et al., 2006), however they also observed cells in the mesangium. Occasional EGFP-positive cells were observed in the adult vascular pole of the *Csf1r–EGFP* transgenic glomeruli, but these appeared to be circulating blood monocytes based upon number, position and morphology (data not shown). Our observations of a trophic role for macrophages (or DCs) during development supports an alternate view to that proposed by Soos et al. (2006). Rather than being an immunological sentinel, we propose that these cells may continue to play a trophic and possibly regenerative role in the postnatal kidney.

Acknowledgments

ML is a Principal Research Fellow and FR is an Industry Fellow with the National Health and Medical Research Council, Australia. We thank Han Chiu and Bree Rumballe for advice and technical assistance, Mike Waters for the provision of rat GH and Melissa Davis and Rohan Teasdale for bioinformatic input. This work was performed as a part of the Renal Regeneration Consortium and was funded by the National Institute for Digestion and Diabetes and Kidney Diseases, NIH (DK63400) and Kidney Health Australia (Bootle bequest). ML is also a Director of Nephrogenix, Pty Ltd.

Appendix A. Supplementary data

Supplementary data associated with this article can be found, in the online version, at doi:10.1016/j.ydbio.2007.05.027.

References

Abe, S., Boyer, C., Liu, X., et al., 2004. Cells derived from the circulation contribute to the repair of lung injury. Am. J. Respir. Crit. Care Med. 170, 1158–1163.

Anderson, M., Anderson, S.K., Farr, A.G., 2000. Thymic vasculature: organizer of the medullary epithelial compartment? Int. Immunol. 12, 1105–1110.

Avner, E.D., Sweeney Jr., W.E., Piesco, N.P., et al., 1985. Growth factor requirements of organogenesis in serum-free metanephric organ culture. In Vitro Cell Dev. Biol. 21, 297–304.

Banaei-Bouchareb, L., Gouon-Evans, V., Samara-Boustani, D., et al., 2004. Insulin cell mass is altered in *Csf1op/Csf1op* macrophage-deficient mice. J. Leukoc. Biol. 76, 359–367.

Berezovskaya, O., Maysinger, D., Fedoroff, S., 1995. The hematopoietic cytokine, colony-stimulating factor 1, is also a growth factor in the CNS: congenital absence of CSF-1 in mice results in abnormal microglial response and increased neuron vulnerability to injury. Int. J. Dev. Neurosci. 13, 285–299.

Bertrand, J.Y., Giroux, S., Golub, R., et al., 2005a. Characterization of purified intraembryonic hematopoietic stem cells as a tool to define their site of origin. Proc. Natl. Acad. Sci. U. S. A. 102, 134–139.

Bertrand, J.Y., Jalil, A., Klaine, M., et al., 2005b. Three pathways to mature macrophages in the early mouse yolk sac. Blood 106, 3004–3011.

Biswas, S.K., Gangi, L., Paul, S., et al., 2006. A distinct and unique transcriptional program expressed by tumor-associated macrophages (defective NF-kappaB and enhanced IRF-3/STAT1 activation). Blood 107, 2112–2122.

Blair, H.C., Robinson, L.J., Zaidi, M., 2005. Osteoclast signalling pathways. Biochem. Biophys. Res. Commun. 328, 728–738.

Briere, N., Ferrari, J., Chailler, P., 1991. Insulin and transferrin restore important cellular functions of human fetal kidney in serum-free organ culture. Biochem. Cell Biol. 69, 256–262.

Carninci, P., Sandelin, A., Lenhard, B., et al., 2006. Genome-wide analysis of mammalian promoter architecture and evolution. Nat. Genet. 38, 626–635.

Chailler, P., Ferrari, J., Briere, N., et al., 1991. Fetal mouse kidney maturation in vitro: coordinated influences of epidermal growth factor, transferrin and hydrocortisone. Anat. Embryol. (Berl.) 184, 319–329.

Challen, G., Gardiner, B., Caruana, G., et al., 2005. Temporal and spatial transcriptional programs in murine metanephric development. Physiol. Genomics 23 (2), 159–171.

Chitu, V., Stanley, E.R., 2006. Colony-stimulating factor-1 in immunity and inflammation. Curr. Opin. Immunol. 18, 39–48.

Cohen, P.E., Chisholm, O., Arceci, R.J., et al., 1996. Absence of colony-stimulating factor-1 in osteopetrotic (*csfmop/csfmop*) mice results in male fertility defects. Biol. Reprod. 55, 310–317.

Dai, X.M., Ryan, G.R., Hapel, A.J., et al., 2002. Targeted disruption of the mouse colony-stimulating factor 1 receptor gene results in osteopetrosis, mononuclear phagocyte deficiency, increased primitive progenitor cell frequencies, and reproductive defects. Blood 99, 111–120.

Dzierzak, E., 2003. Ontogenic emergence of definitive hematopoietic stem cells. Curr. Opin. Hematol. 10, 229–234.

Ekblom, P., Thesleff, I., 1985. Control of kidney differentiation by soluble factors secreted by the embryonic liver and the yolk sac. Dev. Biol. 110, 29–38.

Geutskens, S.B., Otonkoski, T., Pulkkinen, M.A., et al., 2005. Macrophages in the murine pancreas and their involvement in fetal endocrine development in vitro. J. Leukoc. Biol. 78, 845–852.

Gordon, S., Taylor, P.R., 2005. Monocyte and macrophage heterogeneity. Nat. Rev., Immunol. 5, 953–964.

Henson, P.M., Hume, D.A., 2006. Apoptotic cell removal in development and tissue homeostasis. Trends Immunol. 27, 244–250.

Hume, D.A., 2006. The mononuclear phagocyte system. Curr. Opin. Immunol. 18, 49–53.

Hume, D.A., Monkley, S.J., Wainwright, B.J., 1995. Detection of *c-fms* protooncogene in early mouse embryos by whole mount in situ hybridization indicates roles for macrophages in tissue remodelling. Br. J. Haematol. 90, 939–942.

Hume, D.A., Pavli, P., Donahue, R.E., et al., 1988. The effect of human recombinant macrophage colony-stimulating factor (CSF-1) on the murine mononuclear phagocyte system in vivo. J. Immunol. 141, 3405–3409.

Isbel, N.M., Nikolic-Paterson, D.J., Hill, P.A., et al., 2001. Local macrophage proliferation correlates with increased renal M-CSF expression in human glomerulonephritis. Nephrol. Dial. Transplant. 16, 1638–1647.

Kluth, D.C., Erwig, L.P., Rees, A.J., 2004. Multiple facets of macrophages in renal injury. Kidney Int. 66, 542–557.

Le Meur, Y., Leprivey-Lorgeot, V., Mons, S., et al., 2004. Serum levels of macrophage-colony stimulating factor (M-CSF): a marker of kidney allograft rejection. Nephrol. Dial. Transplant. 19, 1862–1865.

Li, W.W., Setzu, A., Zhao, C., et al., 2005. Minocycline-mediated inhibition of microglia activation impairs oligodendrocyte progenitor cell responses and remyelination in a non-immune model of demyelination. J. Neuroimmunol. 158, 58–66.

Lichanska, A.M., Hume, D.A., 2000. Origins and functions of phagocytes in the embryo. Exp. Hematol. 28, 601–611.

Lichanska, A.M., Browne, C.M., Henkel, G.W., et al., 1999. Differentiation of the mononuclear phagocyte system during mouse embryogenesis: the role of transcription factor PU.1. Blood 94, 127–138.

Luo, Y., Zhou, H., Krueger, J., et al., 2006. Targeting tumor-associated macrophages as a novel strategy against breast cancer. J. Clin. Invest. 116, 2132–2141.

Mantovani, A., Sica, A., Sozzani, S., et al., 2004. The chemokine system in diverse forms of macrophage activation and polarization. Trends Immunol. 25, 677–686.

Mantovani, A., Sica, A., Locati, M., 2005. Macrophage polarization comes of age. Immunity 23, 344–346.

Martinez, F.O., Gordon, S., Locati, M., et al., 2006. Transcriptional profiling of the human monocyte-to-macrophage differentiation and polarization: new molecules and patterns of expression. J. Immunol. 177, 7303–7311.

Michaelson, M.D., Bieri, P.L., Mehler, M.F., et al., 1996. CSF-1 deficiency in mice results in abnormal brain development. Development 122, 2661–2672.

Murrell, W., Feron, F., Wetzig, A., et al., 2005. Multipotent stem cells from adult olfactory mucosa. Dev. Dyn. 233, 496–515.

Nishitani, K., Sasaki, K., 2006. Macrophage localization in the developing lens primordium of the mouse embryo – an immunohistochemical study. Exp. Eye Res. 83, 223–228.

Park, J.E., Barbul, A., 2004. Understanding the role of immune regulation in wound healing. Am. J. Surg. 187, 11S–16S.

Piper, M., Wilkinson, L., Nurcombe, V., et al., 2002. Addition of Slit2 protein does not affect ureteric branching during kidney development. Int. J. Dev. Biol. 46 (4), 545–550.

Pull, S.L., Doherty, J.M., Mills, J.C., et al., 2005. Activated macrophages are an adaptive element of the colonic epithelial progenitor niche necessary for regenerative responses to injury. Proc. Natl. Acad. Sci. U. S. A. 102, 99–104.

Roth, P., Stanley, E.R., 1996. Colony stimulating factor-1 expression is developmentally regulated in the mouse. J. Leukoc. Biol. 59, 817–823.

Roth, P., Dominguez, M.G., Stanley, E.R., 1998. The effects of colony-stimulating factor-1 on the distribution of mononuclear phagocytes in the developing osteopetrotic mouse. Blood 91, 3773–3783.

Sasmono, R.T., Oceandy, D., Pollard, J.W., et al., 2003. A macrophage colony-stimulating factor receptor–green fluorescent protein transgene is expressed throughout the mononuclear phagocyte system of the mouse. Blood 101, 1155–1163.

Saxen, L., 1987. Organogenesis of the Kidney. Cambridge University Press, Cambridge.

Shepard, J.L., Zon, L.I., 2000. Developmental derivation of embryonic and adult macrophages. Curr. Opin. Hematol. 7, 3–8.

Sica, A., Schioppa, T., Mantovani, A., et al., 2006. Tumour-associated macrophages are a distinct M2 polarised population promoting tumour progression: potential targets of anti-cancer therapy. Eur. J. Cancer 42, 717–727.

Soos, T.J., Sims, T.N., Barisoni, L., et al., 2006. CX3CR1+ interstitial dendritic cells form a contiguous network throughout the entire kidney. Kidney Int. 70, 591–596.

Stanley, E.R., Berg, K.L., Einstein, D.B., et al., 1997. Biology and action of colony-stimulating factor-1. Mol. Reprod. Dev. 46, 4–10.

Sweet, M.J., Campbell, C.C., Sester, D.P., et al., 2002. Colony-stimulating factor-1 suppresses responses to CpG DNA and expression of toll-like receptor 9 but enhances responses to lipopolysaccharide in murine macrophages. J. Immunol. 168 (1), 392–399.

Sweet, M.J., Hume, D.A., 2003. CSF-1 as a regulator of macrophage activation and immune responses. Arch. Immunol. Ther. Exp. (Warsz) 51, 169–177.

Tagoh, H., Himes, R., Clarke, D., et al., 2002. Transcription factor complex formation and chromatin fine structure alterations at the murine *c-fms* (CSF-1 receptor) locus during maturation of myeloid precursor cells. Genes Dev. 16, 1721–1737.

Turnbull, I.R., Gilfillan, S., Cella, M., et al., 2006. Cutting edge: TREM-2 attenuates macrophage activation. J. Immunol. 177 (6), 3250–3254.

Van Ginderachter, J.A., Movahedi, K., Hassanzadeh Ghassabeh, G., et al., 2006. Classical and alternative activation of mononuclear phagocytes: picking the best of both worlds for tumor promotion. Immunobiology 211, 487–501.

Van Nguyen, A., Pollard, J.W., 2002. Colony stimulating factor-1 is required to recruit macrophages into the mammary gland to facilitate mammary ductal outgrowth. Dev. Biol. 247, 11–25.

Wilson, H.M., Walbaum, D., Rees, A.J., 2004. Macrophages and the kidney. Curr. Opin. Nephrol. Hypertens. 13, 285–290.

Wood, W., Turmaine, M., Weber, R., et al., 2000. Mesenchymal cells engulf and clear apoptotic footplate cells in macrophageless PU.1 null mouse embryos. Development 127, 5245–5252.

Yang, F.M., Friedrichs, W.E., Buchanan, J.M., et al., 1990. Tissue specific expression of mouse transferrin during development and aging. Mech. Ageing Dev. 56, 187–197.

Yoder, M.C., 2001. Introduction: spatial origin of murine hematopoietic stem cells. Blood 98, 3–5.